Human Adenovirus dependent Regulation of Human Endogenous Retroviruses as a Prerequisite for Cancer Development

A thesis submitted in partial fulfilment of the requirements of the

Five Year BS-MS

Dual Degree Program at

Indian Institute of Science Education and Research, Pune

by

Prateek Yadav (20151116)

Biology Division, IISER Pune

Supervisors:

PD Dr. Sabrina Schreiner (Institute of Virology, TUM)

Dr. Michelle Vincendeau (Helmholtz Zentrum Munich)

TAC: **Dr. Sanjeev Galande (IISER Pune)**

CONTENTS

CERTIFICATE

This is to certify that this dissertation entitled "Human Adenovirus dependent Regulation of Human Endogenous Retroviruses as a Prerequisite for Cancer Development" towards the partial fulfilment of the BS-MS dual degree programme at the Indian Institute of Science Education and Research (IISER) Pune, represents study/work carried out by Prateek Yadav at Institute of Virology, Technical University of Munich, Germany under the supervision of PD Dr. rer. nat. Sabrina Schreiner (Institute of Virology, TUM) and Dr. Michelle Vincendeau (Helmholtz Zentrum Munich) during the academic year 2019 – 2020.

Technische Universität München
Research Unit *Antiviral defense of DNA viruses*
Institut für Virologie
Neuherberg 08.04.2020

PD Dr. rer. nat. Sabrina Schreiner,
Institute of Virology, TUM Germany

Prateek Yadav

Dr. Michelle Vincendeau,
Helmholtz Zentrum Munich

DECLARATION

I hereby declare that the matter embodied in the report entitled "Human Adenovirus dependent Regulation of Human Endogenous Retroviruses as a Prerequisite for Cancer Development" are the results of the work carried out by me at the Department of Biology, Institute of Virology, TUM Germany, under the supervision of PD Dr. rer. nat. Sabrina Schreiner (Institute of Virology, TUM) and Dr. Michelle Vincendeau (Helmholtz Zentrum Munich), and the same has not been submitted anywhere else for any other degree.

Technische Universität München
PD Dr. Sabrina Schreiner
Research Unit Antiviral Defense of DNA viruses
Institut für Virologie
GBW 3525, Raum 005
Trogolstädter Landstr. 1
85764 Neuherberg
Tel. +49 89 3187 3490

PD Dr. rer. nat. Sabrina Schreiner,
Institute of Virology, TUM Germany

Prateek Yadav

Dr. Michelle Vincendeau,
Helmholtz Zentrum Munich

ABSTRACT

Human adenoviruses (HAdV) for efficient infection needs to ensure genome decondensation and transcription of viral genes. KAP1 regulates these early stages of infection and is also the main epigenetic factor involved in the repression of human endogenous retroviruses (HERVs).

Upon infection in cell lines like A549, H1299, and HepaRG, SUMOylated KAP1 degrades, and phosphorylation at Serine 824, Serine 473, gets altered. Changes in HERV levels are observed after infection. The expression of HERV-K decreases in A549 cells, whereas the expression of HERV-K and HERV-W increases in H1299 cells. No significant changes were observed in HERV levels in HepaRG cells. For the determination of viral protein involved in HERV modulation, different HAdV mutants were used. We identified the early viral proteins E1B-55K and E4orf6 to be important players in the KAP1 modulation and HERV reactivation.

On the other hand, we observed a change in HERV levels and pluripotency markers in human Induced Pluripotent Stem cells (hIPSc) after infection. Pax6 levels increase, and Nanog level decreases upon infection. KAP1 knockdown in iPS cells leads to a reduction in Pax6 and Nanog expression, whereas an increase in HERV-E expression. From the IFA studies, we speculated increase in Pax6 levels to be related to PML-NBs, which in turn is modulated by E2A or E4orf3. Our work highlights the role of KAP1 and PTMs in regulating HERVs and pluripotency. This study also highlighted the importance of tissue-specific HERV regulation and how adenovirus could transform cells by regulating these processes.

LIST OF FIGURES

LIST OF TABLES

ACKNOWLEDGMENTS

I would like to thank PD Dr. rer. nat. Sabrina Schreiner and Dr. Michelle Vincendeau, for their guidance and continued support in all aspects of the project, throughout my thesis. They gave me the opportunity and vision to work in the area of Virology. Timely discussions and meetings with them have been very fruitful and enlightening. Their insistence on learning from every failed experiment taught me how to be a better investigator. I want to thank Julia Mai and Vidya Padmanabhan Nair for their constant support and insights during this project. I want to thank all the Antiviral Defense of DNA viruses' lab members for their assistance regarding the project and experiments.

I express my sincerest gratitude towards Dr. Sanjeev Galande, IISER Pune, for being the expert member of my Thesis Advisory Committee and also for his valuable suggestions for the project.

I would like to thank the IISER and all the faculty members who have played a vital role in my scientific growth. My stay would not have been possible without the financial support from KVPY Scholarship. I would also thank the Institute of Virology, TUM, and Helmholtz Zentrum Munich for allowing me to carry out my masters' project here. I am thankful to all my friends who were always there and inspired me to work hard. And last but not least, I am grateful to my mother and sisters for always supporting me.

INTRODUCTION

1. Adenoviruses

1.1 Classification

Adenoviruses (AdV) are large (90-100nm), non-enveloped, icosahedral particles with a linear double-stranded (ds) genome of DNA and were initially isolated from adenoids of human (Rowe et al., 1953). AdV can infect a variety of vertebrates and are subdivided into five different genera based on the host they are infecting (Davison et al., 2003):

- *Aviadenoviruses* – Infect birds
- *Atadenoviruses* – Infect mammals, reptiles, birds and contain A+T bases in a high proportion
- *Mastadenoviruses* – Infect mammals
- *Siadenoviruses* – Infect reptiles and birds
- *Ichtadenoviruses* – Infect fishes

Human Adenoviruses (HAdV) belong to the *Mastadenoviridae* genus. This genus is further segregated into seven species HAdV A - G based on their properties of hemagglutination and serum neutralization, their oncogenic potential in rodents and similarity in DNA sequence (Davison et al., 2003; Fields et al., 1993) and are additionally distinguished by their pathogenicity (see Table 1). Species B, -C and -E mainly causes respiratory disease, whereas species A, -D, -F, and -G infect the gastrointestinal tract. Other species like -D and -E can cause ocular defects like endemic and non-endemic keratoconjunctivitis. These viruses cause a wide range of diseases, from the common cold to multi-organ diseases in people with immunodeficiencies (Lion, 2014). HAdV infections may be asymptomatic in immunocompetent patients or lead to mild, local disease, which is usually self-limited by the host. No unique antiviral treatment against HAdVs is safe. Newly evolving HAdV strains, such as HAdV B14p1, have shown lethal results in otherwise stable patients who are not immunosuppressed (Tang et al., 2013).

The most studied HAdV types are the C2 and C5, and they serve as a significant player in vector development (Vetrini and Ng, 2010).

Table 1: Classification of HAdV (Chen and Tian, 2018)

*, the newly named types were from GenBank (http://www.ncbi.nlm.nih.gov/Taxonomy/). I, complete agglutination of monkey erythrocytes; II, complete agglutination of rat erythrocytes; III, partial agglutination of rat erythrocytes; IV, little or no agglutination.

Species	Hemagglutination group	Types	% GC	Associated disease
A	IV	12, 18, 31, 61	47~49	Cryptic enteric infection
B	I	B1: 3, 7, 16, 21, 50, 66, 68	50~52	Conjunctivitis; acute respiratory disease; hemorrhagic cystitis; central nervous system
		B2: 11, 14, 34, 35, 55, 79	50~52	
C	III	1, 2, 5, 6, 57	57~59	Endemic infection; respiratory symptoms
D	II	8~10, 13, 15, 17, 19, 20, 22~30, 32, 33, 36~39, 42~49, 51, 53, 54, 56, 58~60, 62~65, 67, 69, 70, 71, 73, 74, 75	57~60	Keratoconjunctivitis in immunocompromised and AIDS patients
E	III	4	57	Conjunctivitis; acute respiratory disease
F	III	40, 41	57~59	Infantile diarrhea
G	Unknown	52	58	Gastroenteritis
Unclassified	Unknown	72, 76, 77, 78	Unknown	Unknown

1.2 Genomic Structure and Organization

HAdVs are non-enveloped viruses with an approximately 26 - 45 kb linear double-stranded DNA genome (Fields et al., 1993), containing inverted terminal repeats (ITRs) at both ends (Davison et al., 2003). Inverted terminal repeats (ITRs) function as the replication origin site (ORI) (Saha et al., 2014; Vetrini and Ng, 2010). Fig. 1 shows the schematic organization of the HAdV type 5 virion.

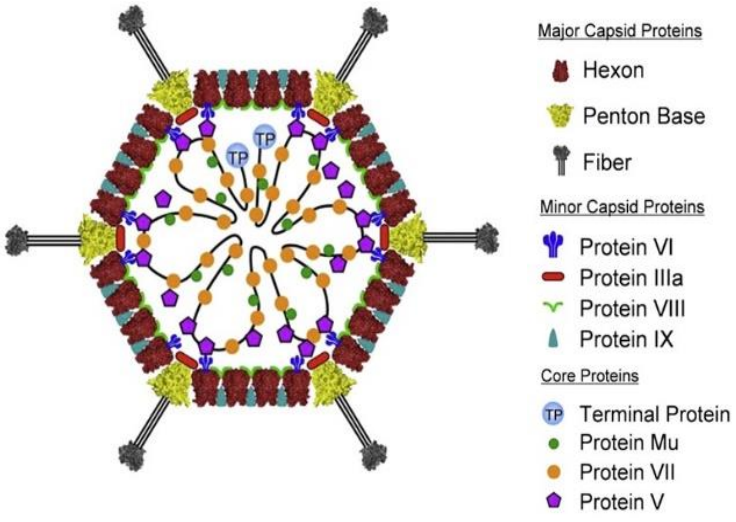

Figure 1: HAdV virion structure. Schematic representation of a HAdV type 5 virion (adapted from (Nemerow et al., 2009)).

The HAdV capsid consists of 240 homotrimeric hexon proteins (viral protein II), forming 20 triangular facets with 12 pentons, comprising of penton bases (viral protein

III) and fibers (viral protein IV) projected at each vertex (Fig. 1). The fiber knob often mediates the virus being bound to the host cell by attaching the Coxsackie and Adenovirus Receptor (CAR). Some viruses (species B), however, use specific receptors for attachment, such as CD46.

The structural proteins are classified into major capsid protein hexon, penton base and fiber, the minor capsid proteins pVI, pIIIa, pVIII, and pIX and the core proteins TP, Mu, pVII, pV, and IVa2 and the viral protease. Minor capsid proteins are involved in the stabilization of the capsid (Nemerow et al., 2009; Saha et al., 2014). The pVI protein stimulates the E1A promoter by suppressing the transcriptional repressor Daxx (Schreiner et al., 2012). Proteins pV, pVII, and Mu are involved in viral DNA condensing inside of the capsid (Nemerow et al., 2009; Saha et al., 2014). Protein IVa2 is involved in DNA packaging (Zhang et al., 2001).

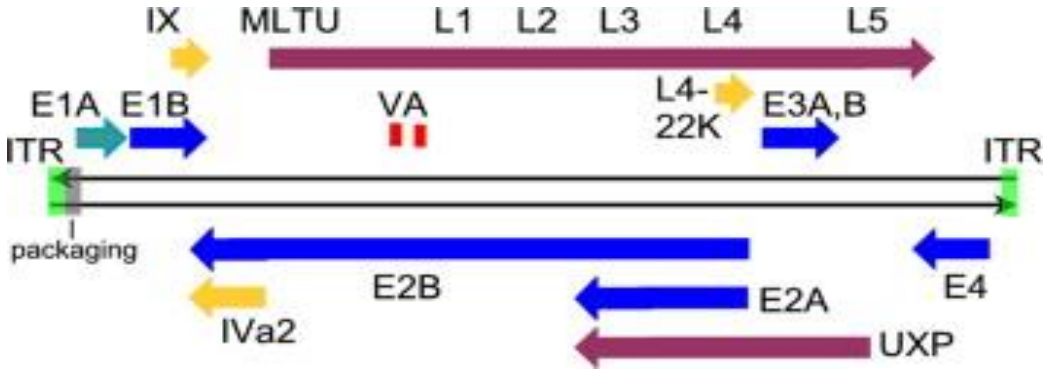

Figure 2: Genome organization of HAdV type 5. Schematic representation of the genome organization of HAdV type 5. Adapted from (Leppard 2014).

The genome of HAdV is divided into nine transcriptional units – five early (E1A, E1B, E2, E3, and E4), three delayed early (IX, IVa2, E2 late) and one major late transcription unit (MLTU), which is processed into five late mRNA families (L1, L2, L3, L4, L5) (Fig. 2) (Leppard, 2014). Early proteins are mostly involved in transcriptional and translational regulation (E1A, E4), viral DNA replication (E2), cell cycle control (E1A) and the modulation of host factors, which are part of the host antiviral immune response (E3) or block of apoptosis (E1B-55K) (Vetrini and Ng, 2010). Host RNA polymerase II synthesizes almost all HAdV C5 mRNAs, while RNA polymerase III transcribes the viral associated (VA) RNAs (Saha et al., 2014).

1.3 Adenoviral Pathogenesis

Human Adenovirus affects mainly the eyes, the genitourinary tract, respiratory, and gastrointestinal tract (Gonçalves and de Vries, 2006). HAdV enters the cell through clathrin-mediated endocytosis initiated by the interaction between the Penton base and integrin (Yousuf et al., 2013). After internalization, endosome acidification is needed for the initiation of HAdV uncoating. The β-hydroxyl group of a serine amino acid in the precursor terminal protein (pTP) of adenovirus, acts as a primer for adenoviral DNA replication (Hoeben and Uil, 2013). The genes first transcribed are genes of the E1A region. It transactivates other genes like E1B, E2, E3, and E4. These genes are involved in the early stages of the HAdV replication cycle (Bos and ten Wolde-Kraamwinkel, 1983). The E2 region codes for proteins such as DNA polymerase, precursor terminal protein (Hoeben and Uil, 2013). The E3 gene region is vital for host defence interaction (Ginsberg et al., 1989). L1 region genes are essential for virion assembly (Ahi and Mittal, 2016), whereas the L3 gene region is involved in the maturation and generation of progeny DNA (Hoeben and Uil, 2013).

1.4 HAdV Oncogenic Potential

Adenovirus transformed cells are virion free, with only two early genes – E1A and E1B-55K being strongly expressed. The primary transformation gene is E1A, while E1B acts as a “helper” gene (Williams et al., 1995). The E1A proteins modulate the role of different proteins that regulate growth. The proteins E1A and E1B prevent apoptotic reaction and induce cell transformation (Debbas and White, 1993). The proteins E1B-55K and E1B-19K obstruct the apoptosis induction capability of p53 (Sarnow et al., 1982; Debbas and White, 1993). Another viral protein, the E4orf6, can also block the ability to start transcription by binding to p53 (Dobner et al., 1996). The protein E1B-55K links to the p53 N-terminal and the E4orf6 protein binds near to the oligomerization domain. E1B-55K acts as a substrate recognition factor, whereas E4orf6 assembles components by connecting Elongin C through BC-box (Sohn and Hearing, 2016). SUMOylation of p53 restricts PML-NBs and leads to the inactivation (Sohn and Hearing, 2016). In short, HAdV E1A, E1B-55K, and E4orf6 are involved in the transformation of cells.

2 Human Endogenous Retroviruses

Endogenous retroviruses account for 8% of the human genome and are retrovirus derived (Mager and Medstrand, 2003). The full-length genomic structure of HERV is shown in Fig. 3. The integrated provirus at the 5' end and 3' end contains the long terminal repeats (LTR), which are needed for retroviral transcription. The genome of

retrovirus consists of majorly three coding areas: gag, pol, and env. In the gag coding region, structural proteins like capsid and nucleocapsid proteins are encoded while envelope proteins are encoded in the env region. Pol region expresses integrase and reverses transcriptase enzymes. Some ERV classes have a more diverse genome and codes for other proteins also. HERV-K (HML2) *env* gene can express two splice variants Np9 and Rec, these two variants have oncogenic properties (Grandi and Tramontano, 2018). HERVs also have a primer-binding site (PBS) between the 5′LTR and *gag,* which binds cellular tRNA and results in (–) DNA strand synthesis (Stoye, 2012).

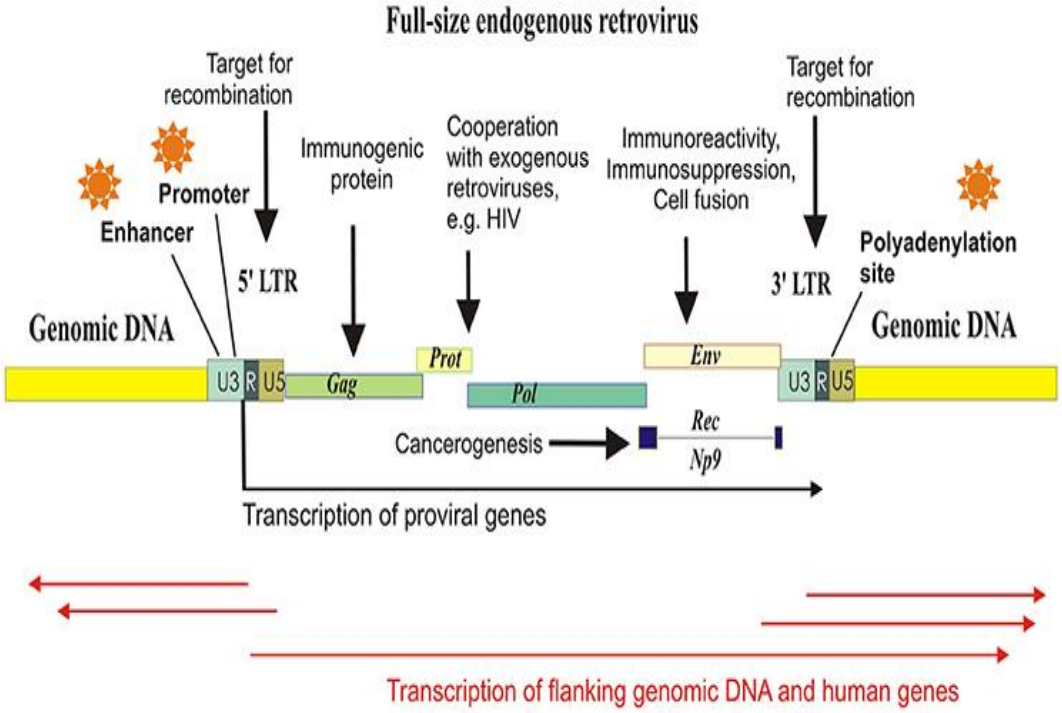

Figure 3: Genome organization of an integrated retroviral provirus. Schematic representation of the structure of an integrated retrovirus (provirus). Adapted from (Buzdin et al., 2017).

HERVs belong to the category of retrotransposons or retroelements. Transposons can alter its location within the genome. Retroelements are often divided into two classes, LTR containing, and one without LTR. HERVs belong to the LTR elements, whereas The Long interspersed nuclear elements (LINEs) and short interspersed elements (SINEs) make the non-LTR class. The human genome phylogenetically comprises at least 31 separate HERV groupings (Katzourakis and Tristem 2005). HERVs were classified initially by homology to exogenous mammalian retroviruses and categorized into three different classes, Class I, II, and III (Fig. 4).

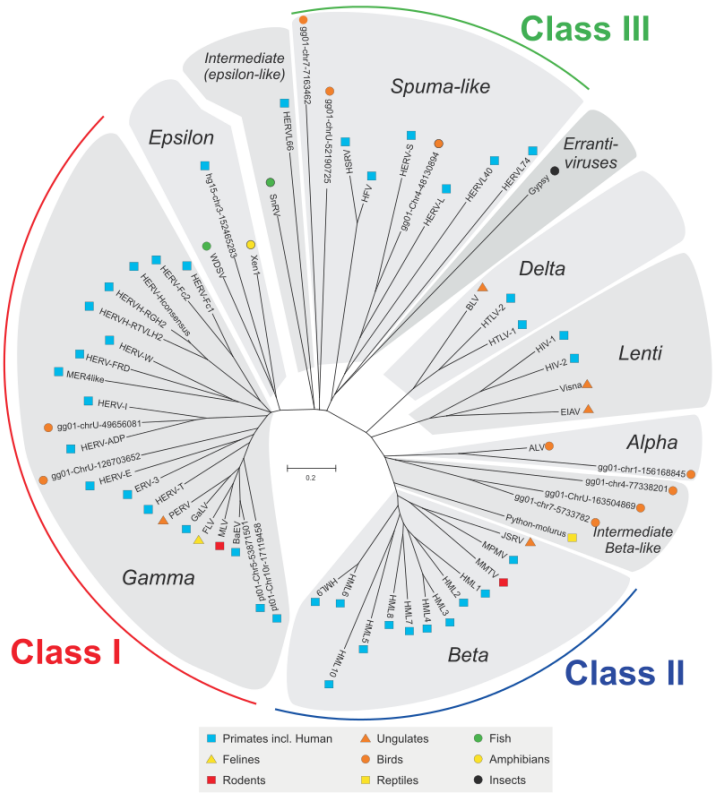

Figure 4: Representative retroviral dendrogram . Unrooted Pol neighbor-joining (NJ) dendrogram of the seven retroviral genera. Adapted from (Jern et al., 2005).

The *Retroviridae* family includes RNA viruses of a positive-sense, single-stranded (ss) type and is subcategorized into *Orthoretrovirinae* and *Spumaretrovirinae*. *Orthoretrovirinae* subfamily has six genera - Alpha, Beta, Gamma, Delta, Epsilon, and Lenti. Traditionally the PBS sequence was used to characterize HERV like HERV-K (lysine tRNA), HERV-W (tryptophan tRNA).

Depending on the specific integration of the HERV families, many of them possess regulatory functions in transcription and can regulate gene expression in human cells. When a HERV provides an additional transcriptional start site (TSS), chimeric transcripts of LTR and gene sequences are produced. When HERVs are integrated into the same transcriptional direction to existing genes, they provide new polyadenylation signals (Baust et al., 2000).

We know that HERVs can perform many molecular functions; it is no wonder that pathological behavior can lead to adverse effects and conditions of serious diseases.

Moreover, they can be reactivated by many factors like exogenous viral infections (Vincendeau et al., 2015). Therefore, HERV sequences should be silenced, and a major player involved in the silencing is the tetrapod-specific KRAB domain-containing zinc finger proteins (KRAB-ZFPs) along with their interaction partner KAP1 (KRAB-associated protein 1) (Iyengar and Farnham, 2011). They silence the sequences by incorporating repressive histone marks and DNA methylation (Stoye, 2012; Suntsova et al., 2015).

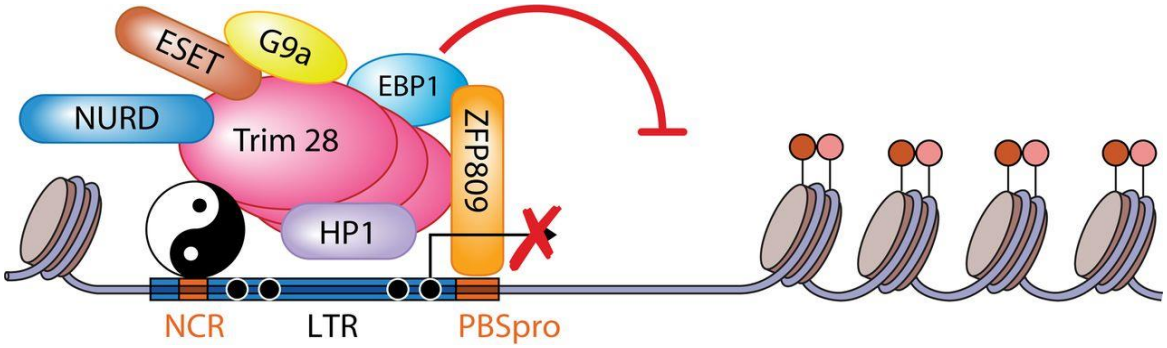

Figure 5: Repression of HERVs. Schematic representation of the repression of HERVs by different factors. Adapted from (Schlesinger and Goff, 2015).

3. KRAB-associated Protein 1 (KAP1)

3.1 KAP1 protein architecture

The KAP1/TRIM28 protein regulates the chromatin organization by influencing epigenetic patterns and chromatin compaction. It engages in several cellular processes like transcriptional regulation, cell growth (Iyengar and Farnham, 2011). KAP1 protein has 835-amino acid and comes from the tripartite motif (TRIM) family (Stoll et al. 2019) (Fig. 6). The PxVxL motif in the KAP1 central region recruits Heterochromatin Protein 1 (HP1), which is needed for transcriptional silencing (Stoll et al. 2019). KAP1 contains a PHD and bromodomain at C-terminal. The SUMO E2 ligase Ubc9 is recruited by PHD and acts as a SUMO ligase by SUMOylating various bromodomain lysines (Stoll et al. 2019). Recruitment of SETDB1 and NuRD requires SUMOylated KAP1 (Stoll et al. 2019).

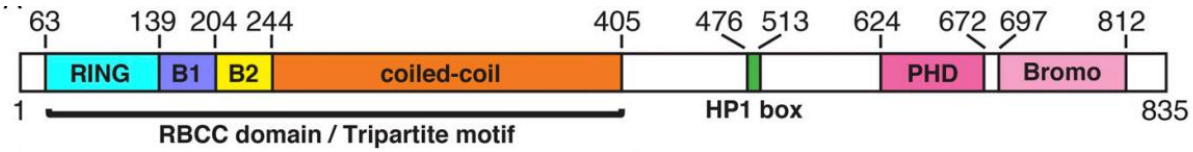

Figure 6: Architecture of the human KAP1 protein. Representation of KAP1 protein architecture. The protein has 835 amino acids. The several domains (RBCC domain, HP1 box, and PB domain) are indicated. Adapted from (Stoll et al. 2019)

3.2 KAP1 transcriptional function

Posttranslational modifications (PTMs), like SUMOylation and phosphorylation, play a crucial role in controlling transcriptional regulation. KAP1 protein undergoes multiple PTMs like SUMOylation and phosphorylation and regulates transcription (Iyengar and Farnham, 2011). KAP1 also participates in apoptosis regulation by integrating HDAC1 into the MDM2-p53 complex and marking p53 for degradation (Iyengar and Farnham, 2011). KAP1 plays a role in DNA repair, too. Ataxia-telangiectasia mutated (ATM), and DNA-dependent protein kinase (DNA-PK) are triggered during DNA damage (Yang et al., 2003). KAP1 phosphorylated at serine 824 co-localizes at damage sites with γH2AX foci (White et al., 2012). KAP1 also undergoes phosphorylation at Serine 473 mediated via Protein Kinase C delta during the cell cycle with the highest amount in late G1, early S phase (White et al., 2012). This modification might interfere with HP1 interaction as this modification is near the HP1 binding domain on KAP1 (Chang et al., 2008). There is no clear evidence of whether KAP1 phosphorylation at Serine 473 is also involved in DNA damage response or chromatin organization (Chang et al., 2008)

4 Role of SUMOylation and cellular proteins during productive HAdV infection

4.1 Modulation of the SUMO conjugation pathway by HAdV

PTMs like ubiquitinylation, phosphorylation, and SUMOylation plays an essential role during various cellular processes such as cell division, immune, and cell cycle control. SUMOylation is a reversible process modification involving a three-step enzymatic cascade, namely activation, conjugation, and substrate modification. Activation consists of the use of the E1 enzyme (Boggio et al., 2004); conjugation is mediated by the E2 enzyme (Lin et al., 2002), whereas the last step involves the cooperation of E2 and E3 ligases (Reverter and Lima, 2005). Viruses exploit these pathways during

infection for the production of higher viral progeny and the evasion from the cellular immune response. Several HAdV early proteins gain some of their functions by crosstalk with the host SUMO system (Sohn and Hearing, 2016). The viral E1B-55K protein serves as a SUMO E3 ligase and stimulates SUMOylation of p53 at PML-NBs (Muller and Dobner, 2008). Another viral protein, E4orf3, is known to SUMOylates cellular proteins like Mre11 and Nbs1. SUMO modification of Mre11 and Nbs1 negatively regulates their DNA Damage Response (DDR) activity (Araujo et al., 2005). E1B-55K recruits RNF4 and together leads to the proteasomal degradation of Daxx and limits its antiviral activity (Zhong et al., 2000). In short, the SUMO pathway plays a crucial role in infection with HAdV.

4.2 Cellular Response during productive HAdV infection

HAdV expresses early viral genes to counteract the antiviral measures for productive infection. HAdV gene expression is negatively regulated by Daxx/ATRX complex (Zhong et al., 2000) and SPOC1 (Bürck et al., 2016). Daxx protein with ATRX induces deacetylation, and SPOC1 is associated with the formation of heterochromatin by interaction with methyltransferases. E1B-55K/E4orf3 inactivates the DDR involved Mre11/RAD50/NBS1 (MRN) complex and allows viral gene replication (Shah and O'Shea, 2015). Upon HAdV infection, KAP1 binds to the early protein E1B-55K and promotes its SUMOylation, which leads to the phosphorylation of KAP1 at Serine 824. It leads to the deSUMOylation of KAP1 and dissociation of the KAP1 repressive complex. E1B-55K/E4orf6 expression after HAdV infection leads to degradation of SPOC1, followed by a reduction of H3K9me3 repressive histone marks (Schreiner et al., 2013).

4.3 Modulation of HERV by KAP1

HERV elements can perform a plethora of functions by providing alternate promoters, enhancers, etc. (Turelli et al., 2014). In early embryos, however, repressive histone marks and DNA methylation hold these elements in the silenced state (Rowe and Trono, 2011). The pathway that is best-known in the repression of HERVs starts with the recognition of the HERV sequence by DNA binding factors, namely KAP1/TRIM28. KAP1 protein recruits SETDB1, NuRD complex, and performs the function of the transcriptional silencing by establishing repressive histone marks and heterochromatin

formation (Stoll et al. 2019). Moreover, KAP1 knockdown leads to the removal of repressive marks placed on retroelements (Turelli et al., 2014). It highlights that KAP1 plays a significant role in regulating HERVs.

4.4 Role of KAP1 during other virus infections

KAP1 has already been shown to play an important role in endogenous retroviruses suppression (Rowe et al., 2010). For the suppression of nonendogenous latent virus-like HIV1, EBV, similar mechanisms are involved. KSHV and HCMV are maintained in the latent stage because of KAP1 (Lieberman 2016). HCMV gets reactivated when KAP1 is present in the phosphorylated form (Rauwel et al., 2015). KSHV latency is further maintained through the modulation of KAP1 by STAT3 (King et al., 2015). These studies suggest that KAP1 plays a very central role in regulating viral latency.

Additionally, it was shown that HAdV combats the histone-based repressive function of KAP1 (Bürck et al., 2016). Recently, HERVs expression were found to be upregulated in some cancers, and HAdV DNA was detected in human brain tumor tissue, human mantle cell lymphoma, and human sarcoma (Kosulin et al., 2007). At the same time, HERV-K integrations in the tumor suppressor gene BRCA2 and the DNA repair gene XRCC1 have been identified in primary human glioma (Misra et al., 2001). Thus, it is crucial to examine the effect of human exogenous viruses such as HAdV on the transcriptional activity of HERVs to enlighten the transcriptional crosstalk and implications in human tumor development.

MATERIALS & METHODS

Cell Culture

HEK293T cells (DuBridge et al., 1987), H1299 cells (Mitsudomi et al., 1991), and A549 cells (Giard et al., 1973) were cultured in Dulbecco's modified Eagle's medium (DMEM) provided with 5% (vol/vol) Fetal Bovine Serum (FBS) (Sigma F2442), 100 µg/ml of streptomycin and 100 U/ml of penicillin at 37°C in a 5% CO2 atmosphere. For HepaRG cells (Gripon et al. 2002), the DMEM medium was supplemented with 5 µg/ml of bovine insulin, and 0.5 µM hydrocortisone also in addition to 10% (vol/vol) FCS/Pen/Strep. Cells were trypsinized (0.05% trypsin) and subcultured when confluent.

Human Induced Pluripotent stem (hiPS) cells were cultured in Essential 8™ Basal Medium and Essential 8™ Supplement (50X) (Thermo Fisher Scientific). IPSC was cultured on recombinant vitronectin (rh VTN-N) coated plates. 1XPBS with 0.5mM EDTA and 5mM NaCl was used to release the cells, which were then dissociated to small clumps for subculturing.

Viral Infection

H5*pg*4100 operated as a virus of the wild-type (wt). H5*pm*4150 bears a frameshift mutation in the open reading frame of E4orf3, H5*pm*4149 and H5*pm*4154 carry stop codons in the open reading frames of E1B-55K and E4orf6, which prevents the expression of E4orf3, E1B-55K, and E4orf6, respectively. For this study, a replication-competent ΔE3 HAdV-C5 virus (Judith) having eGFP expression cassette under the control of CMV promoter, as well as a replication-incompetent GFP expressing HAdV-C5 were also used. HEK293 cells were used to propagate and titrate viruses of all types. After 48 h of infection, cells were harvested for this. Viruses were isolated by lysing cells in liquid nitrogen and water bath by freezing and thawing three times. New HEK293 cells were infected with these viruses, and titer was determined by adenoviral E2A immunofluorescence staining.

For infection of the different cell lines with viruses, the virus was thawed at room temperature. Subsequently, the volume of the viral stock solution necessary for the infection was calculated based on the number of seeded cells, the number of dishes to infect, the multiplicity of infection (MOI) and the titer of viruses as follows:

$$V_{\text{Virus stock}}\,[\mu l] = \frac{\text{cell number} \ * \ (\text{number of dishes} + 1) \ * \ \text{MOI}}{\text{virus titer}}\,[\mu l]$$

Infections were performed at the MOI of 20 or 50 for A549, H1299 cells, at the MOI of 50 or 100 for HepaRG cells. In iPSC, the infection was done in such a way that 50% of the cells are infected. It was confirmed using FACS analysis.

After removing the media from the culture dishes seeded with the corresponding cell line one day before, the viral stock solution was prepared with DMEM without supplements for a total volume of 1 ml per dish. This amount of the virus dilution was then added to the cell cultures in DMEM without supplements. The infection was stopped after one h of incubation. Therefore, the media was removed, and new media with supplements were added to each cell culture dish.

Simultaneously to the viral infection, the mock infection was performed as a negative control. Therefore, after removing the media from the cell cultures dishes seeded with the corresponding cell lines, DMEM without supplements were directly added to the cell cultures. After 1 h of incubation, this media was then replaced by media with supplements.

Lentiviral vector construction and transduction

Lentiviral vectors were constructed by transfecting HEK 293T cells with the plasmid of interest, the Gag-Pol packaging psPAX2 plasmid (Addgene #12259) as well as pMD2.G plasmid expressing VSV-G envelope (Addgene #12260). The transfection mix was prepared as follows: 250 µl Opti-MEM + 2.5 µg lentiviral plasmid (1.5 µg psPAX2 + 1µg pMD2.G) + 1 µg plasmid of interest + 8 µl Transfection reagent. They were mixed and incubated at RT for 30 min and then added to cells. Cells were transfected at 60 - 70% confluency. Viral media was collected 48h post-transfection. The viral media was filtered through a 0.45 µm filter followed by concentration through Amicon column and added to the iPS cells to be transduced with polybrene (4 µg/ml).

shRNA Mediated Knockdown

For the generation of KAP1 knockdown cell lines, the iPS cells were transduced with short hairpin RNA (shRNA) sequence 5′-GGAGTTGGATCTCTCAGAA-3′ expressing

lentiviral vector, which is targeted to the *kap1* at nucleotides 626 to 643. Positive cell selection was made using Puromycin (1 µg/ml).

RNA Extraction and qRT-PCR

RNA from cell samples was extracted with the Qiagen RNeasy Mini Kit, and cDNA was prepared using the Invitrogen SuperScript First-Strand Synthesis System. For Quantitative RT-PCR, LightCycler 480 (Roche) was used. The composition of the qPCR mix for each sample is as follows: 5 µL of SYBR Green Master Mix (Roche), 1 µL of cDNA and 1 µl of 10µM of the respective primers (forward + reverse). The PCR condition used is the following: At 95°C for 10 min and 45 cycles of 10 s at 95°C, 5 s at 60°C and 10s at 72°C. For the analysis, the obtained viral mRNA levels were determined with respect to the cellular RNA Polymerase II mRNA levels.

Table 2: List of primers used in the study

Primer No.	**Description**	**Sequence (5'-3')**
1)	KAP1 – F KAP1 – R	GCAACATTGCAGAAGAGCACCAAG ACGGCCCCGCTTATTCAGCTC
2)	HERV-K HML 2 – F HERV-K HML 2 – R	GGCCATCAGAGTCTAAACCACG CTGACTTTCTGGGGGTGGCCG
3)	HERV-E – F HERV-E – R	GCTTTCTTTCTGATCCTAGGCTGTG CTTTGGGGAGGCGTTGGCTCGAGACC
4)	HERV-W – F HERV-W – R	TGAGTCAATTCTCATACCTG AGTTAAGAGTTCTTGGGTGG
5)	HERV-H – F HERV-H – R	TGGTGCCGTGACTCGGAT GCTGAGTCCGAAAAGAGAGTC
6)	HERV-T – F HERV-T - R	CCCCTACCCTTTTTGGGG GTACCCCAGGTAGGAAACTCTGGG
7)	RNA Pol-II – F RNA Pol-II – R	GCACCACGTCCAATGACAT GTCGGCTGCTTCCATAA
8)	Hexon – F Hexon – R	CGCTGGACATGACTTTTGAG GAACGGTGTGCGCAGGTA
9)	Pax6 – F	GTGTCCAACGGATGTGTGAG

	Pax6 - R	CTAGCCAGGTTGCGAAGAAC
10)	Nanog – F Nanog – R	TGGGATTTACAGGCGTGAGCCAC AAGCAAAGCCTCCCAATCCCAAAC
11)	Oct-4 – F Oct-4 – R	GGGCTCTCCCATGCATTCAAAC CACCTTCCCTCCAACCAGTTGC

Western Blotting

Cells were scraped in radioimmunoprecipitation assay (RIPA) lysis buffer (150 mM NaCl, 50 mM Tris–HCl/pH 8.0, 5 mM EDTA, 0.1% sodium dodecyl sulphate, 1 mM DTT, 0.5% sodium deoxycholate, 0.1% Triton X-100, 1% Nonidet P-40) containing 0.1% (v/v) aprotinin, 1 mg/ml pepstatin, 1% (v/v) PMSF and 1 mg/ml leupeptin,. To homogenize the cell lysates, the lysates were sonicated for 30 s with a Sonifier 450 (40 pulses, 0.8 pulses/s, 80% output), which was precooled to 5°C. The lysate was centrifuged at 13000g at 4° C for 10 min. Protein content was quantified using Bradford assay (BioRad Smart Spec Plus Spectrophotometer). Samples were prepared in 1X Laemmli buffer (20% glycerol, Tris– HCl/pH 6.8, 0.2% bromophenol blue, 2% SDS, and 0.025% β-mercaptoethanol) by boiling at 95°C and 50 µg protein was loaded. SDS-PAGE was used to resolve protein samples and was transferred to the nitrocellulose membrane. Blocking was done using 5% skimmed milk in 1X PBS for 1h at RT. Primary antibodies were diluted in 1X PBS-T (0.1% Tween 20, Tris buffer saline) and were incubated overnight. Secondary antibodies were diluted in 3% milk in 1X PBS-T. The bands were visualized by enhanced chemiluminescence.

Table 3: List of Antibodies used in Western Blotting

1º Antibodies	**Animal**	**Dilution**	**Supplier**
E1B-55K	Mouse, 2A6	1:10	(Sarnow et al., 1982)
E4orf6	Rabbit, RSA3	1:10	(Marton et al., 1990)
E4orf3	Rat, 6A-11	1:10	(Nevels et al., 1999)

E2A-72K	Mouse, B6-8	1:10	(Reich et al., 1983)
ß-actin	Mouse, AC-15	1:5000	Sigma-Aldrich
KAP1	Mouse, sc-515790	1:1000	Santa Cruz Biotechnologies, Inc.
Phosphorylated KAP1 at Serine 824	Rabbit	1:1000	Bethyl Laboratories
Phosphorylated KAP1 at Serine 473	Rabbit, ab133225	1:1000	abcam
p53	Rabbit, FL-393	1:1000	Santa Cruz Biotechnologies, Inc.
SPOC1	Rabbit, cr56	1:1000	(Kinkley et al., 2009)

Horseradish peroxidase (HRP) conjugated secondary antibodies were used for the detection of proteins. Antibodies used were anti-rabbit IgG (1:10000), anti-mouse IgG (1:10000) and anti-rat IgG (1:10000) (Jackson/Dianova).

Immunofluorescence Assay

For IFA, the iPS cells were grown on coverslips. Cells were washed with 1X PBS twice after 72 hr of infection and then fixed with 4% PFA for 15 min at RT. Cells were washed with 0.15% TritonX-100 for 10 min and permeabilized with 0.3% TritonX-100 for 10 min. Cells were blocked with 5% BSA/0.15% TritonX-100 for 1 h at RT. Cells were washed in 0.15% TritonX-100, followed by incubation in primary antibody diluted in 1X PBS overnight at 4°C in a humidified chamber. Coverslips were washed twice in 0.15% TritonX-100 to remove excess primary antibody. Coverslips were incubated with secondary antibody diluted in 1X PBS for 1 h at RT in a humidified chamber. Secondary antibodies Alexa 488 (Invitrogen) or Alexa 594 (Invitrogen), raised against two different species, were mixed in required concentrations and used. Coverslips were washed once with 0.15% TritonX-100 and stained with DAPI (0.5µg/µl in 2X

FA/SSC) for 30 min at RT. Coverslips were washed twice in 0.15% TritonX-100, and the Zeiss Axiovert 200M microscope was used for imaging.

Table 4: List of antibodies used for IFA

1ºAntibodies	**Animal**	**Dilution**	**Supplier**
E1B-55K	Mouse	1:10	(Sarnow et al., 1982)
E2A	Mouse	1:10	(Reich et al., 1983)
PML	Rabbit	1:100	abcam
Pax6	Rabbit	1:100	BioLegends
E4orf3	Rat	1:200	(Nevels et al., 1999)

RESULTS

To investigate the regulation of HERVs in human cells by HAdV-*wt* infection, different human cancer cell lines were selected, such as A549 (Human lung adenocarcinoma epithelial cell line), HepaRG (Pseudo-primary human hepatoma cell line), and H1299 (Human Non-Small Cell Lung Carcinoma cell line). As a first approach, these cell lines were infected with a certain MOI, and infected cells were harvested at different time points. Western blot analysis was performed for monitoring different protein levels and PTMs of KAP1. qRT-PCR was done to detect transcript levels of HERV. For the regulation of HERV families by adenoviral infection, we decided to analyze three HERV families, namely HERV-K, HERV-W, and HERV-H. HERV-H was taken as KAP1 does not regulate it, whereas KAP1 regulates HERV-K. HERV-W is analyzed because it has been found upregulated in many tumors.

1. HAdV-*wt* infection influences KAP1 PTMs and HERV levels in cancer cells:

Since PTMs of KAP1 play a crucial role in regulating HERV expression, and upon HAdV-*wt* infection, KAP1 PTMs got altered, we investigated the possible reactivation of various HERVs during adenoviral infection. HAdV-*wt* infection was done at MOIs of 20 and 50 in A549 cells. Harvesting of cells was done at different time points 16, 24, 48, and 72 h.p.i (hours post-infection). Two separate biological replicates were used for experiments.

Western blot analysis showed a productive infection of virus treated A549 cells since the adenoviral early protein E1B-55K could be initially detected at 16 h.p.i (Fig. 7, lane 2, 3). Additionally, we can see an increase in E1B-55K protein levels as the infection progresses and with higher MOI. On the contrary, the uninfected mock control did not show any signal for E1B-55K throughout the whole experiment (Fig. 7, lane 1, 4, 7, and 10). The protein level of KAP1 was decreasing as the infection progresses compared to uninfected samples at time points, 48 h.p.i, and 72 h.p.i (Fig. 7, lane 8, 9, 11, and 12). Previous studies demonstrated that p53 is SUMOylated and proteasomal degraded at later stages of HAdV-*wt* infection, so we decided to stain for p53 to confirm the productive infection by HAdV-*wt* through modulation of the tumor suppressor p53. At later stages in infection, we can see an additional band at around 20kDa above p53, the SUMOylated form of p53 (Fig. 7, lane 6, 8, 9, 11, and 12). Furthermore, unmodified p53 was shown to be degraded during infection (Fig. 7, lane

7 – 12). KAP1 protein can be phosphorylated at multiple sites, and we focused on two major phosphorylation sites S473 and S824, which play an essential role during gene expression regulation. The protein level of phosphorylated KAP1 indicated by pKAP1S473 increases in starting at 16 and 24 h.p.i (Fig.7, lanes 1-6) but decreases during the infection compared to the mock control of A549 (Fig. 7, lanes 8 – 12). As previously reported (Bürck et al., 2016), upon HAdV-*wt* infection, KAP1 gets phosphorylated at Serine 824 in response to DDR. We can see that at later stages of infection protein level of pKAP1S824 increases compared to mock controls (Fig. 7).

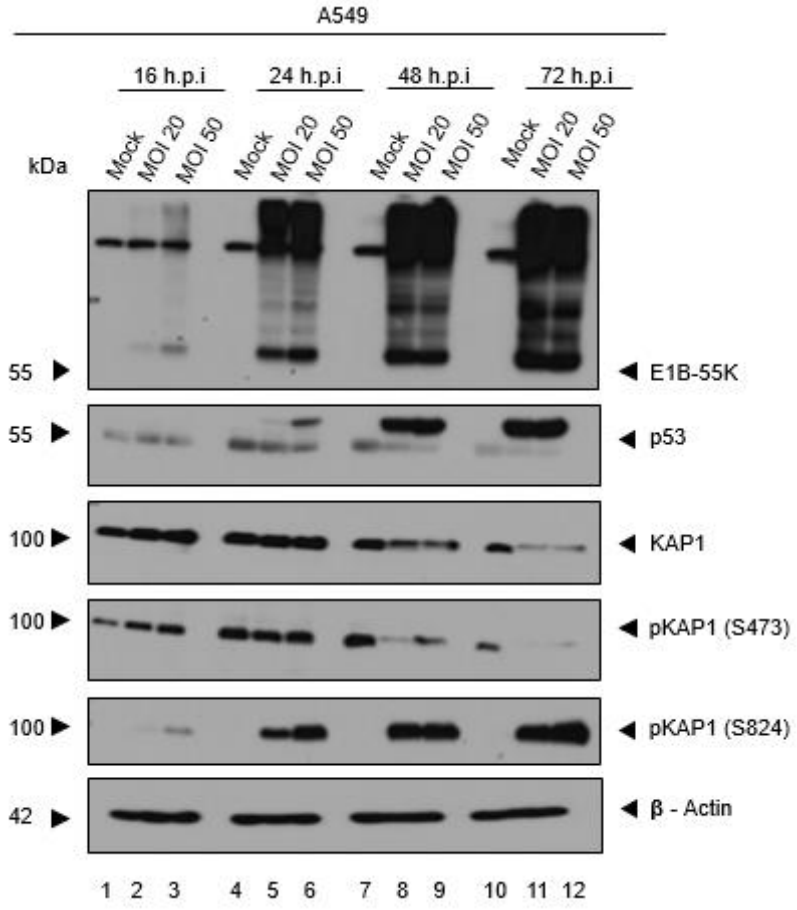

Figure 7: HAdV-*wt* infection influences KAP1 PTMs in A549 cell line. A549 cells were seeded and infected with HAdV-*wt*. Proteins resolved by SDS-PAGE were detected using mouse MAb 2A6 (anti-E1B-55K), mouse polyclonal anti-KAP1, rabbit polyclonal Ab pKAP1S473, rabbit polyclonal pKAP1S824, rabbit polyclonal anti-p53 and mouse MAb AC-15 (β-actin) as a loading control. To assign the molecular weights of the proteins a protein marker was used. Molecular weights are displayed in kDa on the left side. For each cell line and time point $n = 2$.

A)

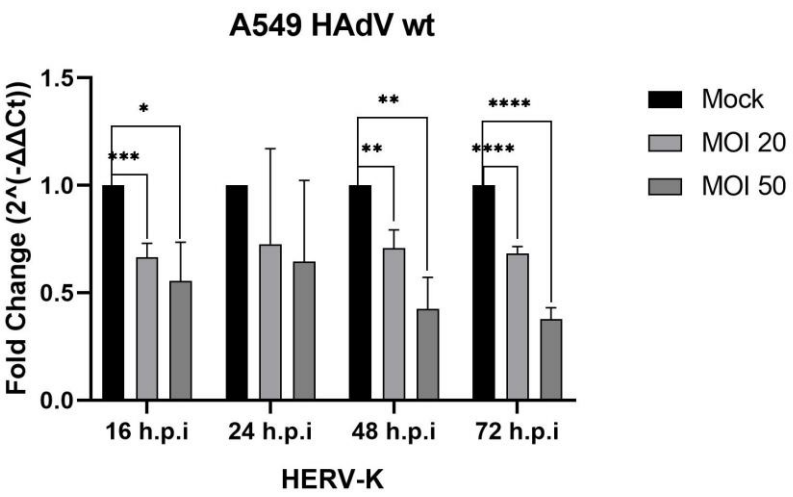
A549 HAdV wt
Fold Change (2^(-ΔΔCt))
1.5
1.0
0.5
0.0
*
***
**
**
****
****
16 h.p.i
24 h.p.i
48 h.p.i
72 h.p.i
HERV-K
Mock
MOI 20
MOI 50

B)

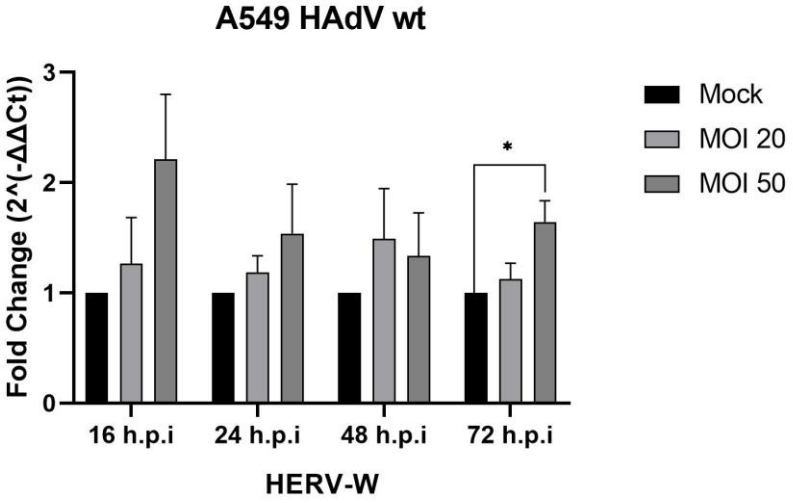
A549 HAdV wt
Fold Change (2^(-ΔΔCt))
3
2
1
0
*
16 h.p.i
24 h.p.i
48 h.p.i
72 h.p.i
HERV-W
Mock
MOI 20
MOI 50

C)

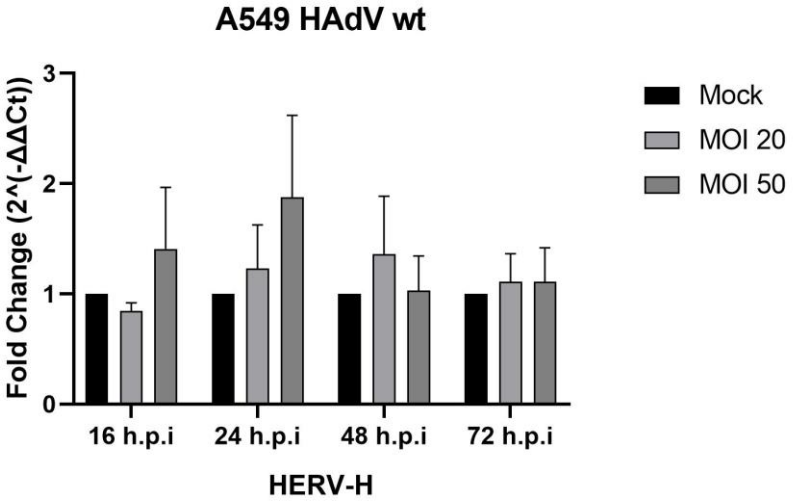
A549 HAdV wt
Fold Change (2^(-ΔΔCt))
3
2
1
0
16 h.p.i
24 h.p.i
48 h.p.i
72 h.p.i
HERV-H
Mock
MOI 20
MOI 50

Figure 8: HAdV-*wt* infection influences HERV levels in A549 cell lines. A) HERV-K B) HERV-W C) HERV-H. The qRT-PCR study was used to assess the level of mRNA upon infection by HAdV-*wt*. The graph depicts fold change (2^ (-ΔΔCt)) in mRNA levels normalized to untreated cells. Significance calculated using unpaired t test. (* = p<0.05, ** = p<0.01, ***p < 0.001, ****p < 0.0001). Error bars – SEM, n=2 biological replicates, n=4 technical replicates. RNA Pol II served as an internal control.

From the qPCR results, we observed that there is no statistically significant change in HERV-H levels upon infection compared to uninfected control (Fig. 8C). In contrast, there is a considerable decrease in HERV-K levels upon infection (Fig. 8 A). As the infection progresses, HERV-K levels keep on decreasing significantly except for 24 hr. The HERV-K expression drops more than 0.5 folds upon infection compared to uninfected mock, and it falls more as MOI increases like for MOI 50 and 72 h.p.i, the expression is 0.3 folds compared to the mock control (Fig. 8A). For HERV-W, there is an almost two-fold increase in expression after 72 hours and MOI 50; otherwise, there is no statistically significant change in HERV-W levels (Fig. 8B).

Since in A549 cells, we saw that upon HAdV-*wt* infection, KAP1 PTMs get altered. Previously, it has been shown that the p53 protein hinders the activity of some HERV LTRs (Chang et al. 2007). So, we wanted to investigate what will happen to KAP1 PTMs and HERVs regulation when there is no p53, and H1299 does not express p53. So, H1299 cells were also infected and harvested, similar to A549 cells. Two independent biological replicates were used for the experiment.

Western blot analysis showed a productive infection of virus treated H1299 cells since the adenoviral early protein E1B-55K could be initially detected at 24 h.p.i for MOI 50 (Fig. 19, lane 6), and it keeps on increasing as the infection progresses (Fig. 19). E1B-55K could not be detected in uninfected mock controls as expected (Fig. 19, lane 1, 4, 7, and 10). We can see a decrease in the KAP1 and an increase in S824 phosphorylated KAP1 protein level as the infection progresses as previously reported when we compare the infected samples to the uninfected mock controls (Fig. 9). We can observe that protein levels of pKAP1S473 decreases upon infection (Fig. 9) in HAdV-wt infected cells similar to that of A549 cells (Fig. 7).

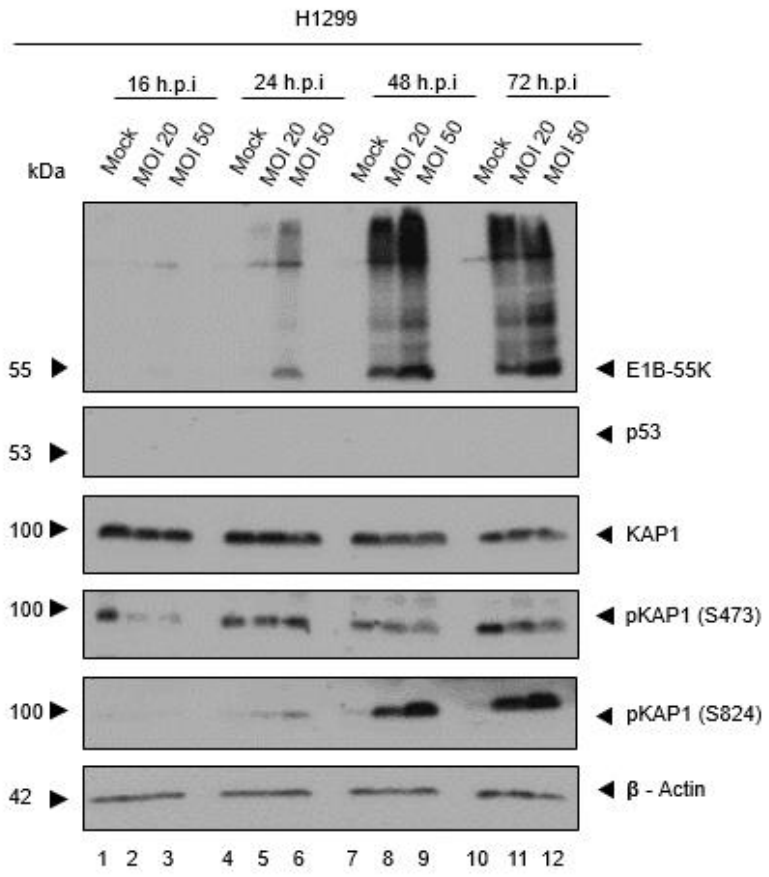

Figure 9: HAdV-*wt* infection influences KAP1 PTMs in H1299 cell line. H1299 cells were seeded and infected with HAdV-*wt*. Proteins resolved by SDS-PAGE were detected using mouse MAb 2A6 (anti-E1B-55K), mouse polyclonal anti-KAP1, rabbit polyclonal Ab pKAP1S473, rabbit polyclonal pKAP1S824, rabbit polyclonal anti-p53 and mouse MAb AC-15 (β-actin) as a loading control. To assign the molecular weights of the proteins a protein marker was used. Molecular weights are displayed in kDa on the left side. For each cell line and time point $n = 2$.

For Real-time qPCR, cellular mRNA was isolated from uninfected and infected cells, and cDNA was generated.

We observe that just like in A549 cells, HERV-K levels decrease significantly after 16 h.p.i, but contrary to A549 cells, HERV-K levels increase in H1299 cells after 16 h.p.i with a maximum increase at 48 h.p.i. (~1.5 - 2 folds) (Fig. 10A). There is a significant increase (~1.5 folds) in HERV-H levels upon infection after 24 h.p.i (Fig. 10C), but at other time points, there is no statistically significant change observed. We can see that at 16 h.p.i HERV-W levels significantly decrease (0.6 folds) (Fig. 10C), but as the infection progresses, the expression increases (~ 1.5 folds) at 48 h.p.i (Fig. 10B).

A)

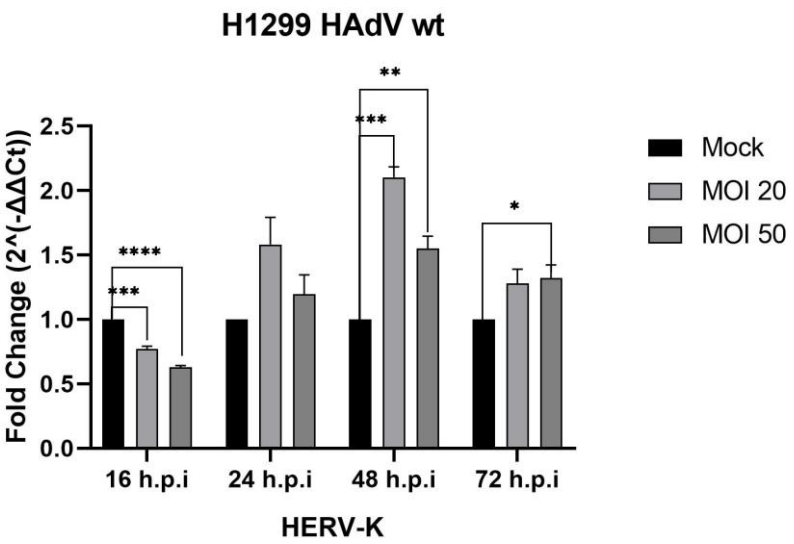
H1299 HAdV wt
Fold Change (2^(-ΔΔCt))
2.5
2.0
1.5
1.0
0.5
0.0
****
***
**
***
*
16 h.p.i
24 h.p.i
48 h.p.i
72 h.p.i
HERV-K
Mock
MOI 20
MOI 50

B)

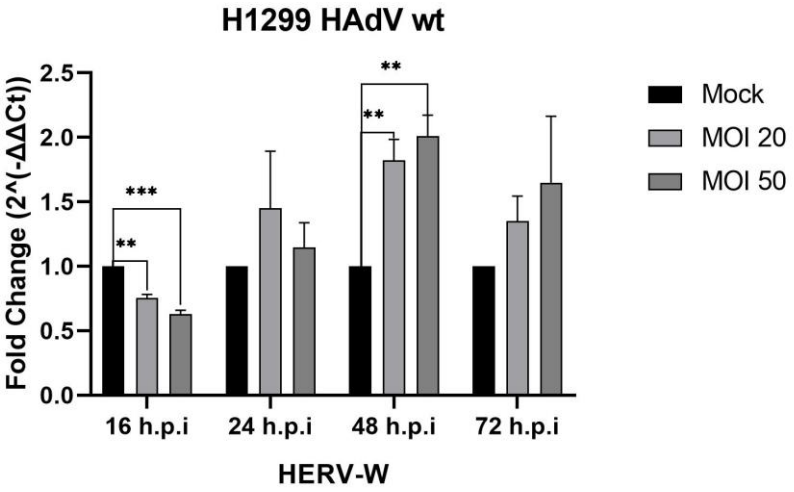
H1299 HAdV wt
Fold Change (2^(-ΔΔCt))
2.5
2.0
1.5
1.0
0.5
0.0
***
**
**
**
16 h.p.i
24 h.p.i
48 h.p.i
72 h.p.i
HERV-W
Mock
MOI 20
MOI 50

C)

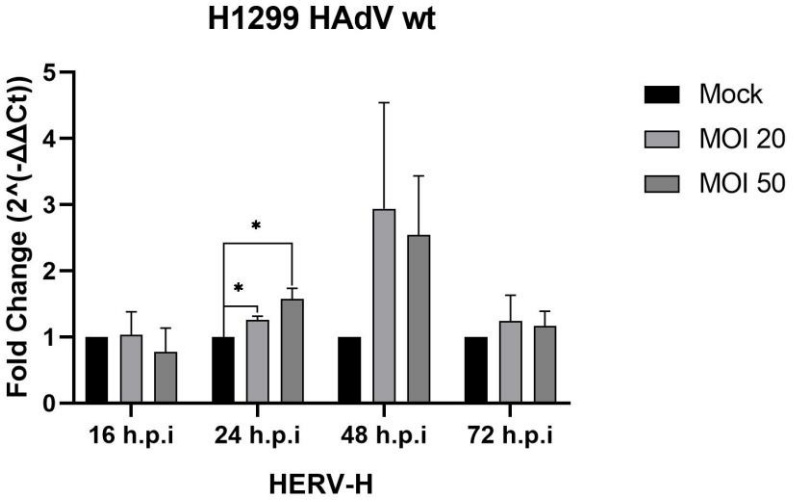
H1299 HAdV wt
Fold Change (2^(-ΔΔCt))
5
4
3
2
1
0
*
*
16 h.p.i
24 h.p.i
48 h.p.i
72 h.p.i
HERV-H
Mock
MOI 20
MOI 50

Figure 10: HAdV-*wt* infection influences HERV levels in H1299 cell lines. A) HERV-K B) HERV-W C) HERV-H. The qRT-PCR study was used to assess the level of mRNA upon infection by HAdV-*wt*. The graph depicts fold change (2^ (-ΔΔCt)) in mRNA levels normalized to untreated cells. Significance calculated using unpaired t test. (* = p<0.05, ** = p<0.01, ***p < 0.001, ****p < 0.0001). Error bars – SEM, N=2 biological replicates, n=4 technical replicates. RNA Pol II was served as internal control.

We investigated the influence of HAdV-*wt* infection on KAP1 PTMs and possible reactivation in two lung carcinoma cell lines, either expressing p53 (A549) or being depleted for p53 (H1299). The activity of endogenous retroviruses is cell type-specific and regulated differently (Seifarth et al. 2005). So, we decided to infect a hepatic cell line, namely HepaRG. It has been already shown that HAdV- *wt* infection in HepaRG progresses differently than A549 and H1299. In HepaRG, infection is slightly delayed, and cytoplasmic aggregates are formed by E1B-55K (Schreiner et al. 2010). We wanted to check what will be the influence of HAdV-*wt* infection on KAP1 PTMs and possible reactivation of HERVs in a hepatic cancer cell line. To this end, HepaRG cells were infected with MOIs of 50 and 100 and harvested at four different time points.

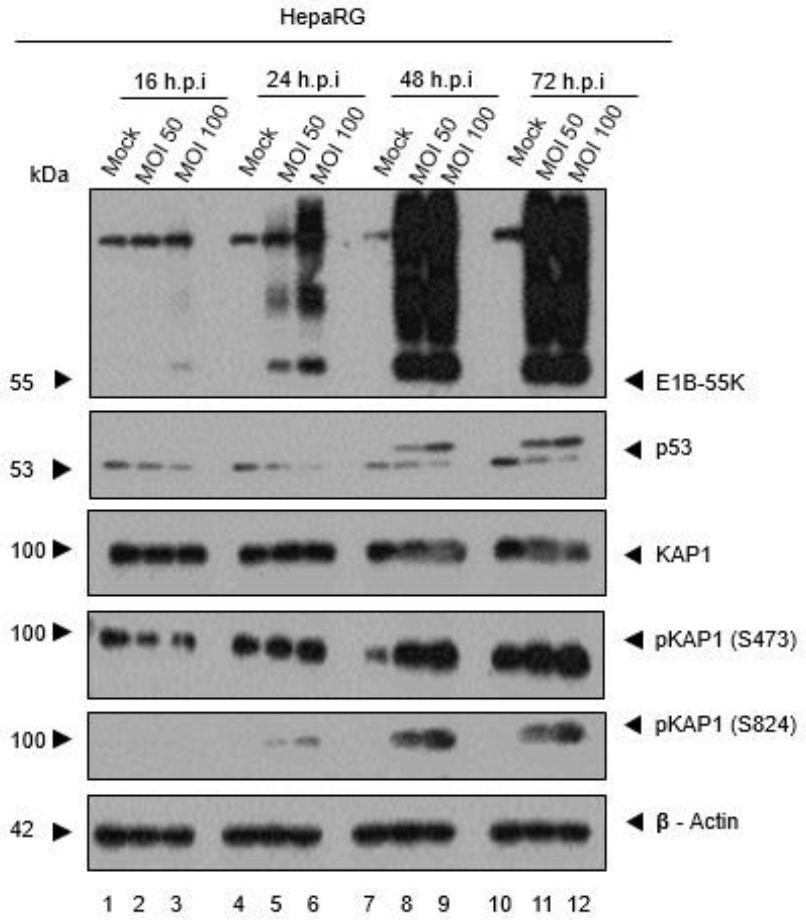

Figure 11: HAdV- *wt* infection influences KAP1 PTMs in HepaRG cell line. HepaRG cells were seeded and infected with HAdV - *wt*. Proteins resolved by SDS-PAGE were detected using mouse MAb 2A6 (anti-E1B-55K), mouse polyclonal anti-KAP1, rabbit polyclonal Ab pKAP1S473, rabbit polyclonal pKAP1S824, rabbit polyclonal anti-p53 and mouse MAb AC-15 (β-actin) as a loading control. To assign the molecular weights of the proteins a protein marker was used. Molecular weights are displayed in kDa on the left side. For each cell line and time point $n = 2$.

Western blot analysis showed a productive infection of virus treated HepaRG cells since the adenoviral early protein E1B-55K could be detected, and the intensity level of E1B-55K protein bands are increasing for higher MOI and later time points (Fig. 11, lanes 5, 6, 8, 9, 11 and 12). On the contrary, the uninfected mock control did not show any signal for E1B-55K throughout the whole experiment (Fig. 11). As already reported, upon infection, p53 is SUMOylated and undergoes proteasomal degradation. We can observe that just like A549 (Fig. 7), there is an additional band above p53 in lanes 8, 9, 11, and 12, approximately 20kDa higher, which represents the SUMOylated form of p53 (Fig. 11). The change in protein levels of the KAP1 and pKAP1 (S824) during infection is similar to that observed in A549 (Fig. 7) and H1299 (Fig. 9). Interestingly, pKAP1 (S473) levels are increasing upon infection, when compared to mock samples, which might be due to the different DDR pathways or genomic architecture of hepatic cells (Fig. 11).

For real-time qPCR, mRNA was isolated, and cDNA was generated.

A)

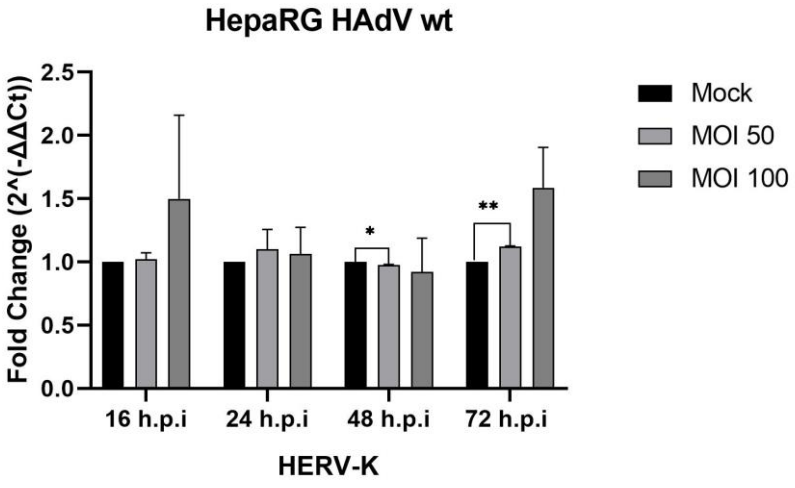

B)

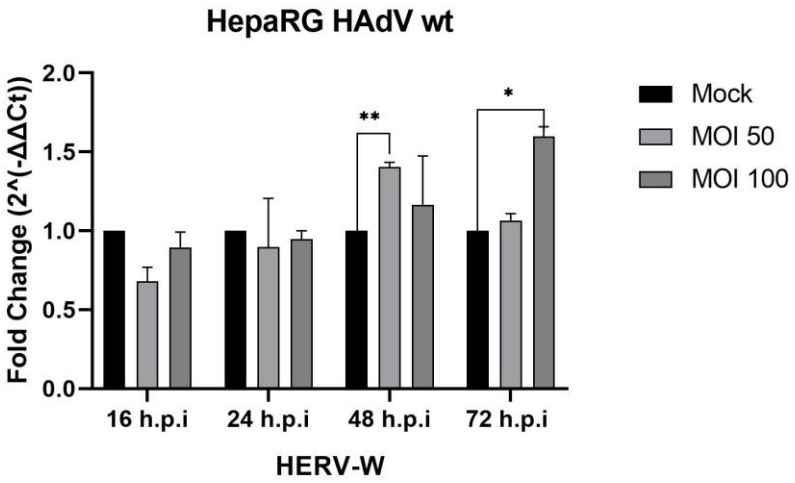

C)

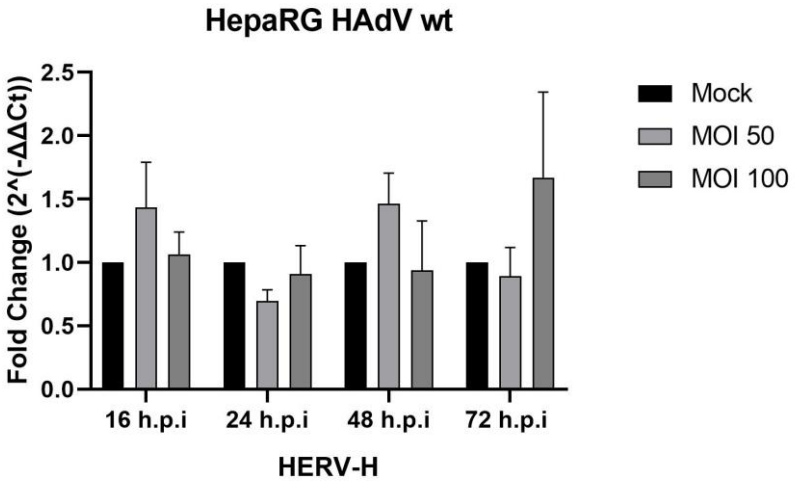

Figure 12: HAdV-*wt* infection influences HERV levels in HepaRG cell line. A) HERV-K B) HERV-W C) HERV-H. The qRT-PCR study was used to assess the level of mRNA upon infection by HAdV - *wt*. The graph depicts fold change (2^ (-ΔΔCt)) in mRNA levels normalized to untreated cells. Significance calculated using unpaired t test. (* = p<0.05, ** = p<0.01). Error bars – SEM, N=2 biological replicates, n=4 technical replicates. RNA Pol II was served as internal control.

From the qRT-PCR graphs, we can see that there is no statistically significant change in HERV-H expression levels upon infection (Fig. 12 C). For HERV-W, there is a slight increase (~1.5 folds) after 48 and 72 h.p.i (Fig. 12 B); otherwise, there is not much change in expression when compared to mock. Contrary to A549 (Fig. 8A), HERV-K expression level in HepaRG slightly increases (~1.2 folds) after 48 and 72 h.p.i for MOI 50 (Fig. 12 A).

2. HAdV mutants infection influences KAP1 PTMs and HERV levels in cancer cells:

As we already know that KAP1 PTMs is mainly modulated by E1B-55K, so we wanted to monitor E1B-55K deletion in the viral background to check its influence on KAP1. We also wanted to investigate other adenoviral regulator proteins for their capacity to target KAP1 and HERV expression as many viral proteins interact with each other and carry out the functions like degradation of KAP1, p53. For this, we tested already generated HAdV variants with depletions in various regulating viral genes to investigate their ability to target KAP1 and molecular background of HERV modulation during infection in the same cell lines. For this, we used different HAdV null mutants like ΔE1B-55K, ΔE4orf3, and ΔE4orf6. The cell lines were infected at a certain MOI, 50 for A549 and H1299, and 100 for HepaRG. Later time points of 48 and 72 h.p.i were selected for analysis. Western blot analysis was performed for monitoring different protein levels and PTMs of KAP1. To detect the transcript levels of HERVs, qPCR was performed.

To determine the influence of a HAdV mutant's infection on KAP1 PTMs as well as on HERV families, A549 cells were infected with HAdV mutants and *wt* at a MOI of 50.

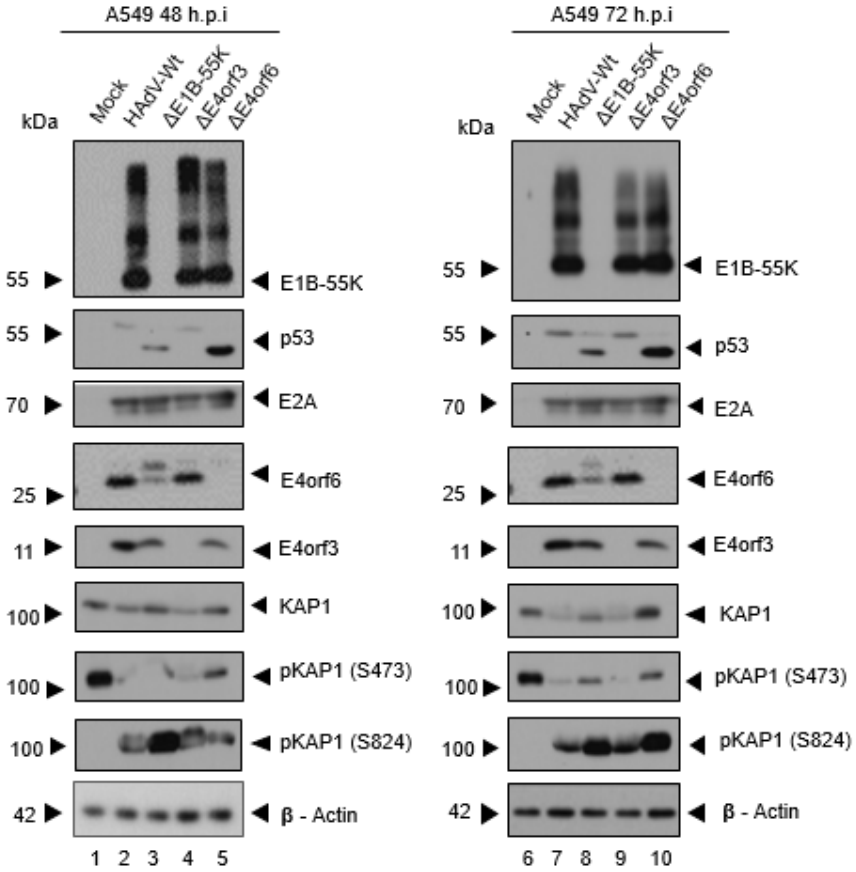

Figure 13: HAdV mutants' infection changes KAP1 PTMs in A549 cell line. A549 cells were seeded and infected with different HAdV mutants at a MOI of 50. Proteins resolved by SDS-PAGE were detected using mouse MAb 2A6 (anti-E1B-55K), mouse polyclonal anti-KAP1, rabbit polyclonal Ab pKAP1S473, rabbit polyclonal pKAP1S824, rabbit polyclonal anti-p53, mAb RSA3 (α-E4orf6), mAb B6-8 (α-E2A), mAb6A11 (α-E4orf3), and mouse MAb AC-15 (β-actin) as a loading control. To assign the molecular weights of the proteins a protein marker was used. Molecular weights are displayed in kDa on the left side. For each cell line and time point *n* = 2.

Western blot analysis showed infection by different virus mutants. Similar levels of E2A in all viruses show that an equal amount of virus was used for infection. From the western blot, we can confirm the virus mutants since the respective band is absent in each mutant. E1B-55K band is missing in the ΔE1B-55K virus, similarly for E4orf3 and E4orf6 (Fig. 13). We can see that p53 is getting SUMOylated in wt (Fig. 13 lanes 2, 7) and ΔE4orf3 samples and unSUMOylated form getting degraded (Fig. 13 lanes 4, 9) as an upcoming band can be observed when compared to uninfected mock (Fig. 13 lanes 1, 6). In ΔE1B-55K (Fig. 13 lanes 3, 8) and ΔE4orf6 (Fig. 13 lanes 5, 10), no SUMOylated p53 can be observed. The protein level of KAP1 can be seen decreasing in wt (Fig. 13 lanes 2, 7) and ΔE4orf3 (Fig. 13 lanes 4, 9), but not in ΔE1B-55K (Fig. 13 lanes 3, 8) and ΔE4orf6 (Fig. 13 lanes 5, 10) when compared to uninfected mock (Fig. 13 lanes 1, 6). The protein level of phosphorylated KAP1 indicated by pKAP1 (S473) follows the same trend as KAP1 with a decrease in wt and ΔE4orf3 background. The protein level of pKAP1 (S824) increases in the absence of E1B-55K (Fig. 13 lanes 3, 8) and E4orf6 (Fig. 13 lanes 5, 10).

For real-time qPCR, mRNA was isolated, and cDNA was generated.

A)

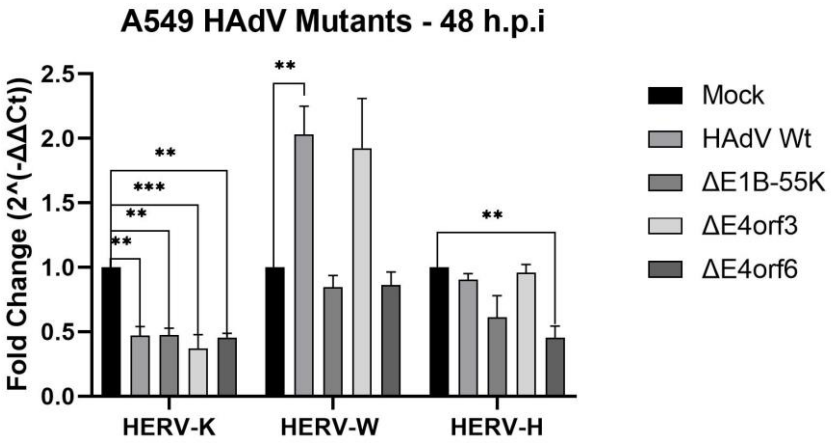

B)

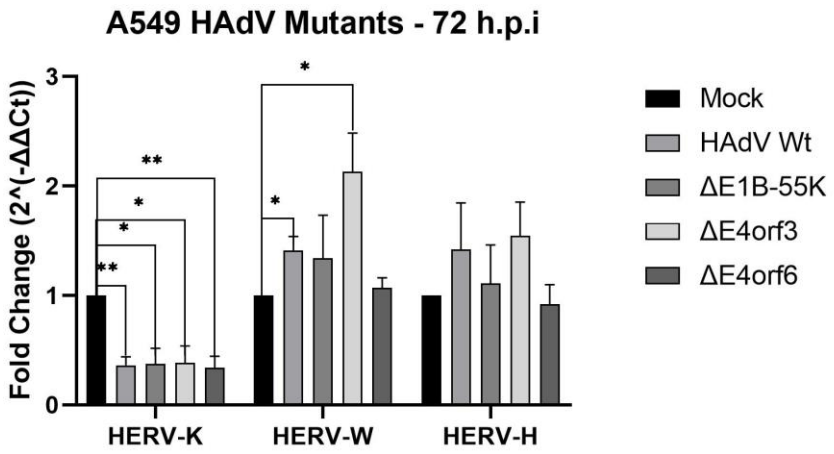

Figure 14: HAdV mutants' infection influences HERV levels in A549 cell line. A) 48 h.p.i B) 72 h.p.i. The qRT-PCR study was used to assess the level of mRNA upon infection by HAdV. The graph depicts fold change (2^ (-ΔΔCt)) in mRNA levels normalized to untreated cells. Significance calculated using unpaired t test. (* = p<0.05, ** = p<0.01, ***p < 0.001). Error bars – SEM, N=2 biological replicates, n=4 technical replicates. RNA Pol II was served as internal control.

Upon infection by virus mutants, HERV-K levels are significantly lower (~0.3 folds) in all mutants when compared to mock controls (Fig. 14). There is not a significant change in HERV-H levels upon infection by virus mutants except for a decrease at 48 h.p.i in the ΔE4orf6 (Fig. 14 A). For HERV-W, a significant increase can be observed upon wt infection at 48 h.p.i (~2 folds) and 72 h.p.i (~1.5 folds) and in ΔE4orf3 at 72 h.p.i (~2 folds) compared to mock controls (Fig. 14).

We know that E4orf6 protein and E1B-55K blocks the ability of p53 to activate transcription, and E1B-55K protein is required for the KAP1 SUMOylation, which leads to disruption of KAP1/SPOC1 complex. To determine the influence of a HAdV mutant's infection on KAP1 PTMs as well as on HERV families in p53 null background, H1299 cells were infected with HAdV-*wt* and mutants at a MOI of 50. From the HAdV-*wt* infection in H1299 cells, we could not observe any significant change in HERV-H levels, so we wanted to check another HERV family. We investigated HERV-T as it has been shown that Human Cytomegalovirus infection upregulates HERV-T (Assinger et al. 2013), and higher expression of HERV-T is found in cancer cells (Yi and Kim 2007). So, along with HERV-K and HERV-W, HERV-T was also investigated.

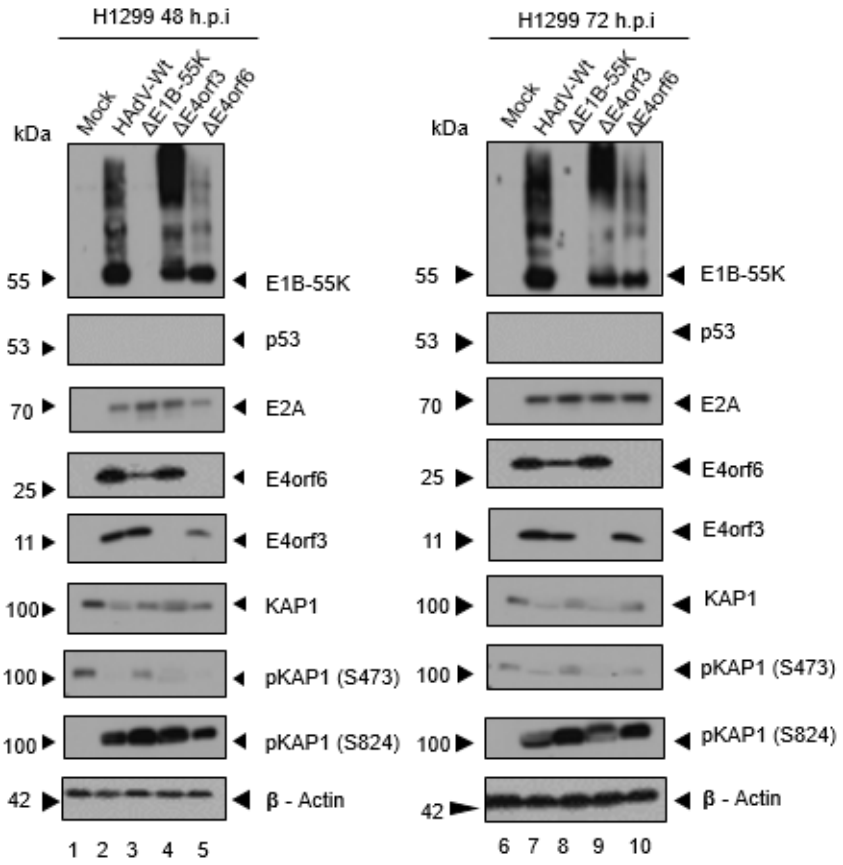

Figure 15: HAdV mutants' infection changes KAP1 PTMs in H1299 cell line. H1299 cells were seeded and infected with different HAdV mutants at a MOI of 50. Proteins resolved by SDS-PAGE were detected using mouse MAb 2A6 (anti-E1B-55K), mouse polyclonal anti-KAP1, rabbit polyclonal Ab pKAP1S473, rabbit polyclonal pKAP1S824, rabbit polyclonal anti-p53, mAb RSA3 (α-E4orf6), mAb B6-8 (α-E2A), mAb6A11 (α-E4orf3), and mouse MAb AC-15 (β-actin) as a loading control. To assign the molecular weights of the proteins a protein marker was used. Molecular weights are displayed in kDa on the left side. For each cell line and time point $n = 2$.

From the western blot, we can confirm each virus mutant and also establish that all the viruses are equal in amount because of similar E2A levels. Similar to A549 (Fig. 13), we can see that KAP1 protein degrades in HAdV-*wt* (Fig. 15 lanes 2, 7) and ΔE4orf3 (Fig. 15 lanes 4, 9) compared to uninfected mock (Fig. 15 lanes 1, 6). The phosphorylated form of KAP1, pKAP1 (S473), similar to KAP1 protein, decreases in wt and ΔE4orf3 background. The protein level of pKAP1 (S824) increases in the absence of E1B-55K (Fig. 15 lanes 3, 8) and E4orf6 (Fig. 15 lanes 5, 10) compared to mock (Fig. 15 lanes 1, 6).

For real-time qPCR, mRNA was isolated, and cDNA was generated.

A)

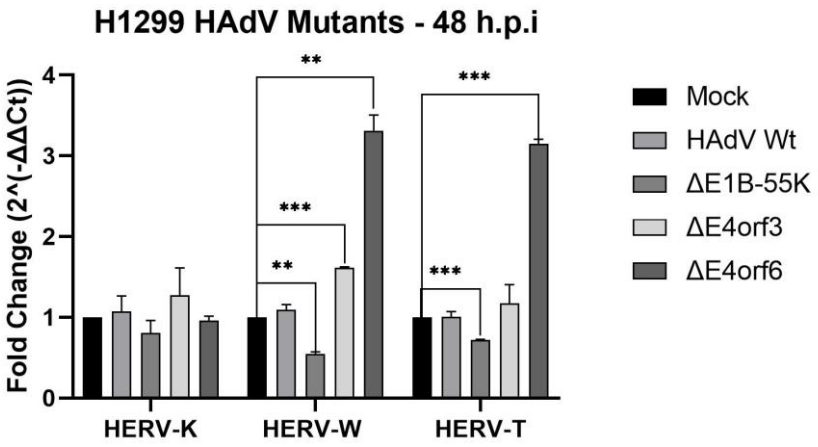

B)

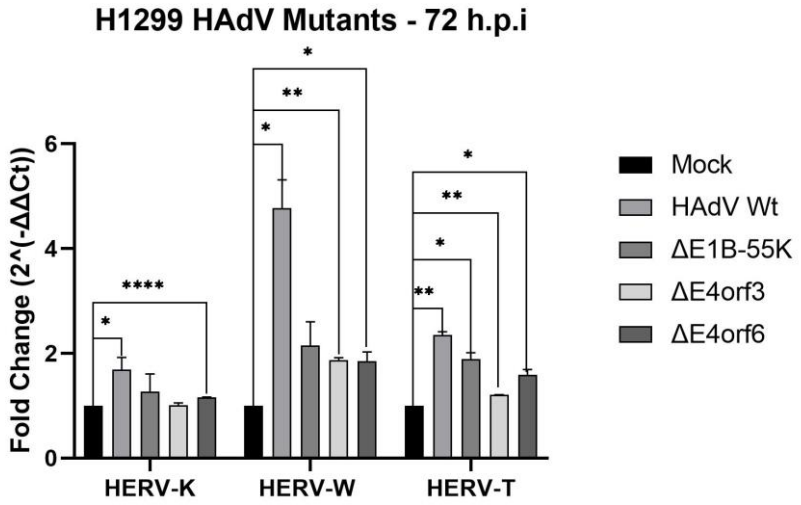

Figure 16: HAdV mutants' infection influences HERV levels in H1299 cell line. A) 48 h.p.i B) 72 h.p.i. The qRT-PCR study was used to assess the level of mRNA upon infection by HAdV. The graph depicts fold change (2^ (-ΔΔCt)) in mRNA levels normalized to untreated cells. Significance calculated using unpaired t test. (* = p<0.05, ** = p<0.01, ***p < 0.001, ****p < 0.0001). Error bars – SEM n=2 biological replicates, n=4 technical replicates. RNA Pol II was served as internal control.

In H1299 cells, upon infection by virus mutants, we can see a significant increase in the expression level of HERV-K in the wt (~1.8 folds) and E4orf6 mutant background (~1.3 folds) at 72 h.p.i (Fig. 16 B). We can observe a change in HERV-W expression levels upon infection by HAdV mutants. HERV-W and HERV-T expression levels are majorly increasing upon infection. After 48 h.p.i, there is a decrease in HERV-W (~0.5 folds) and HERV-T (~0.8 folds) expression levels in ΔE1B-55K background compared to uninfected mock (Fig. 16 A). There is a more than three-fold increase in the HERV-W and HERV-T levels in ΔE4orf6 infection after 48 h.p.i. (Fig. 16 A). After 72 h.p.i, there is an increase in HERV-W (~4 folds) and HERV-T (~2.2 folds) expression levels upon HAdV-*wt* infection compared to uninfected mock (Fig. 16 B).

We used two lung carcinoma cell lines, one expressing p53 (A549) and one not (H1299) to gain functional insight on adenoviral regulator proteins on KAP1 PTMs modulation and HERV activation. Here, we wanted to check what would be the effect of HAdV regulatory proteins on KAP1 PTMs as well as on HERV families in p53 expressing Hepatic cell line. For this, HepaRG cells were infected with HAdV mutants and *wt* at a MOI of 100.

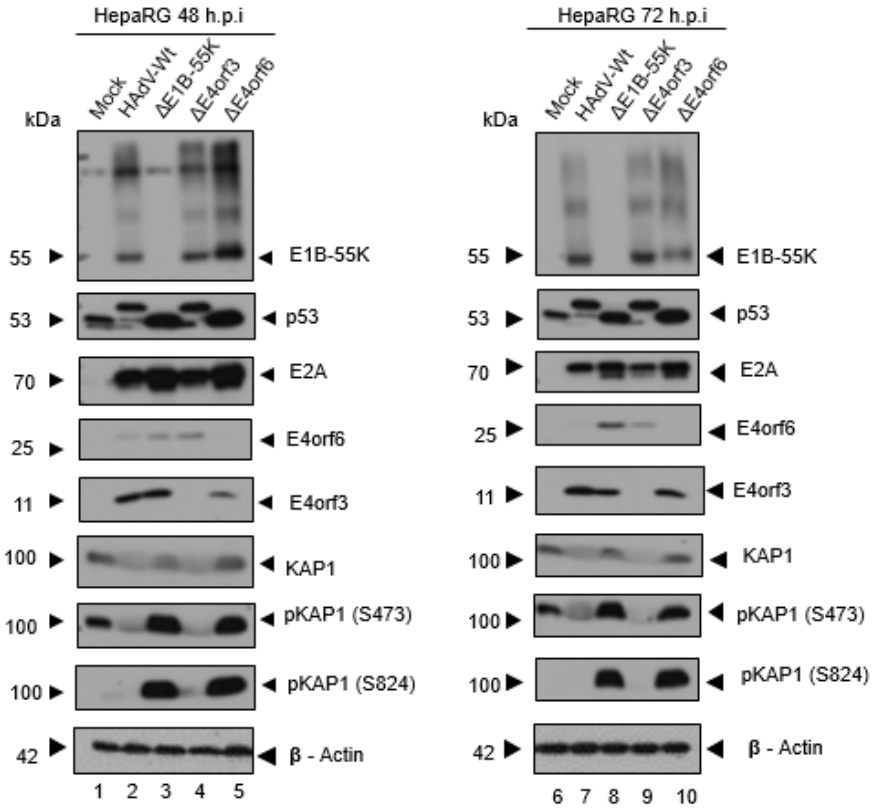

Figure 17: HAdV mutants' infection changes KAP1 PTMs in HepaRG cell line. HepaRG cells were seeded and infected with different HAdV mutants at a MOI of 100. Proteins resolved by SDS-PAGE were detected using mouse MAb 2A6 (anti-E1B-55K), mouse polyclonal anti-KAP1, rabbit polyclonal Ab pKAP1S473, rabbit polyclonal pKAP1S824, rabbit polyclonal anti-p53, mAb RSA3 (α-E4orf6), mAb B6-8 (α-E2A), mAb6A11 (α-E4orf3), and mouse MAb AC-15 (β-actin) as a loading control. To assign the molecular weights of the proteins a protein marker was used. Molecular weights are displayed in kDa on the left side. For each cell line and time point $n = 2$.

Western blot analysis showed an active infection by different virus mutants because of similar E2A protein levels. We can see that p53 is getting SUMOylated and unSUMOylated p53 getting degraded in wt (Fig. 17 lanes 2, 7) and ΔE4orf3 samples (Fig. 17 lanes 4, 9) as an upcoming band can be observed when compared to uninfected mock (Fig. 17 lanes 1, 6). In ΔE1B-55K (Fig. 17 lanes 3, 8) and ΔE4orf6 (Fig. 17 lanes 5, 10), no SUMOylated p53 can be observed. The protein level of KAP1 can be seen decreasing in wt (Fig. 17 lanes 2, 7) and ΔE4orf3 (Fig. 17 lanes 4, 9),

similar to A549 (Fig. 13). The protein level of phosphorylated KAP1 indicated by pKAP1 (S473) follows the same trend as KAP1 with a decrease in wt and ΔE4orf3 background. The protein level of pKAP1 (S824) increases in the absence of E1B-55K (Fig. 17 lanes 3, 8) and E4orf6 (Fig. 17 lanes 5, 10).

For real-time qPCR, mRNA was isolated, and cDNA was generated.

A)

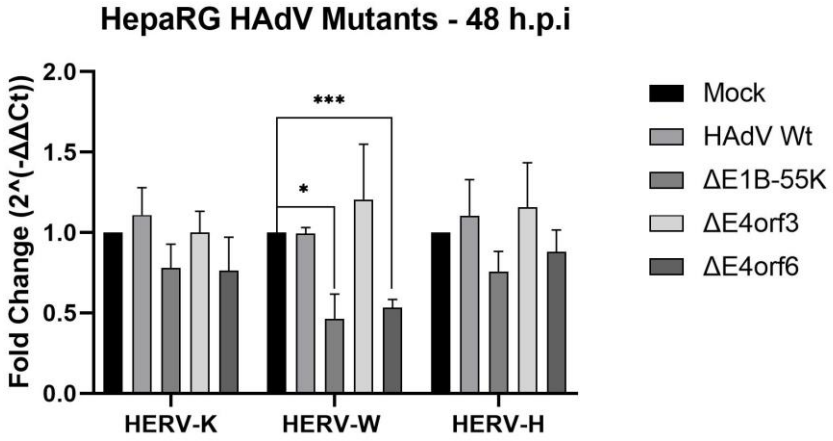

B)

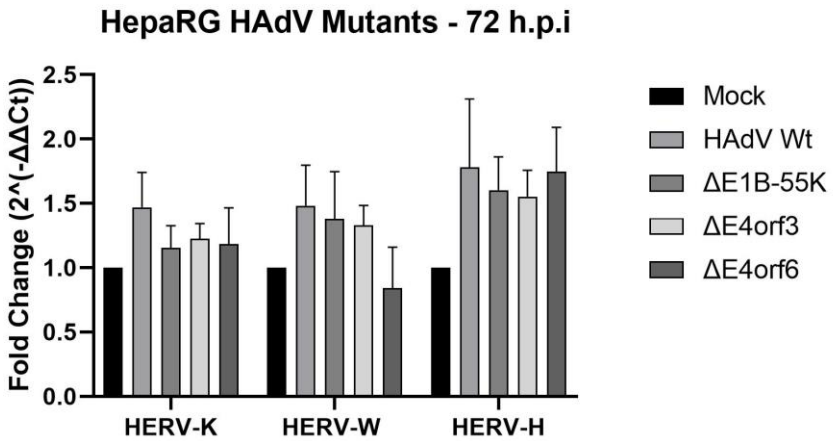

Figure 18: HAdV mutants' infection influences HERV levels in HepaRG cell line A) 48 h.p.i B) 72 h.p.i. The qRT-PCR study was used to assess the level of mRNA upon infection by HAdV. The graph depicts fold change (2^ (-ΔΔCt)) in mRNA levels normalized to untreated cells. Significance calculated using unpaired t test. (* = p<0.05, ** = p<0.01, ***p < 0.001). Error bars – SEM, N=2 biological replicates, n=4 technical replicates. RNA Pol II was served as internal control.

From the qPCR graphs, we can observe that there is not a statistically significant change in HERV levels upon HAdV-*wt* and mutant infections at 72 h.p.i (Fig. 18 B). The most notable difference is the decrease in HERV-W levels (~0.5 folds) after 48 h.p.i in ΔE1B-55K and ΔE4orf6 background compared to uninfected mock (Fig. 18 A).

3. Analysis of HAdV infectivity in Human Induced Pluripotent Stem Cells

It has been shown that KAP1 controls HERVs in early embryonic development (Rowe et al., 2010). HERVs are crucial in the reprogramming of human-induced pluripotent stem cells (hiPSCs) (Matteucci et al. 2018) and also critical to stem cell genome organization (Santoni et al. 2012). To gain more insight in KAP1 and HERV regulation, we decided to use the human induced pluripotent stem cells as its chromatin is more relaxed than differentiated cell lines.

3.1 Comparison of infectivity of different HAdV

To gain insight into how adenovirus modulates KAP1 PTMs, HERV expression, and pluripotency markers in human iPS cells, we infected these cells with GFP expressing replication-competent HAdV (Judith). Judith was used to determining the infection percentage by measuring GFP positive cells (Fig. 19) using flow cytometry. The final working amount was decided in such a way that more than half of the cells are infected, which was around MOI 3000.

After establishing the cell number and viral load of Judith, iPS cells were infected with three different types of viruses, namely Judith, wt, and replication-incompetent Ad5-GFP. Replication incompetent virus was used to check if the onset of virus replication is essential for modulation of KAP1 and HERV levels. To compare the infectivity of all three types of viruses, Immunofluorescence studies were performed. E1B-55K and E2A, two viral proteins, and PML nuclear bodies (PML-NBs) were stained.

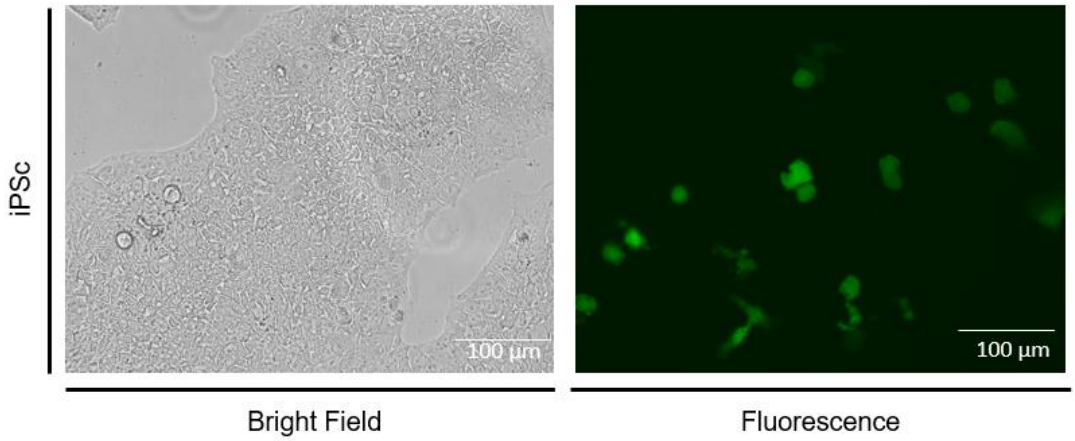

Figure 19: HAdV-GFP positive iPS cells. Representative image of living HAdV-GFP positive iPS cells after 72 h.p.i with MOI 200 and 50,000 cells. The panels are bright field (Left) and fluorescent signals (Right) images for iPSc infected by HAdV-GFP. Imaging was done on EVOS FL Imaging System (Scale bar: 100 µm)

E2A is a marker for viral replication centers. HAdV replication centers are located next to PML-NBs (Fig. 20 B). PML-NBs ranges from five to 15 per nucleus in cell-lines (Lallemand-Breitenbach and de Thé 2018). *Pml* expression is enhanced in HSCs and decreases upon differentiation, and also the number of PML-NBs in HSCs is higher compared to committed cells (Nakahara et al. 2014). Previously, it has been shown that upon infection by HAdV, dot-like PML-NBs are disrupted by early protein E4orf3, reorganizing PML-NBs into track-like structures (Doucas et al. 1996). Furthermore, HAdV places the sites of replication and transcription close to PML tracks, utilizing different factors to enhance efficient viral replication or targeting components of PML-NBs to inhibit their restrictive function (Stubbe et al., 2020). We can observe these track-like structures in infected cells (Fig. 20 C). E1B-55K protein forms a complex with E4orf6 (Sarnow et al. 1984), and the localization of E1B-55K in infected cells is mostly nuclear or near the nucleus (Sarnow et al. 1982). In infected cells, we can observe E1B-55K as red patches in the nucleus (Fig. 20 A). We cannot see any staining in Ad5-GFP virus infection for E1B-55K and E2A as this virus is replication-incompetent (Fig. 20, third panel (Ad5-GFP)). The localization patterns of E1B-55K, E2A, and PML in infected cells look similar in both HAdV-*wt* and Judith virus.

A)

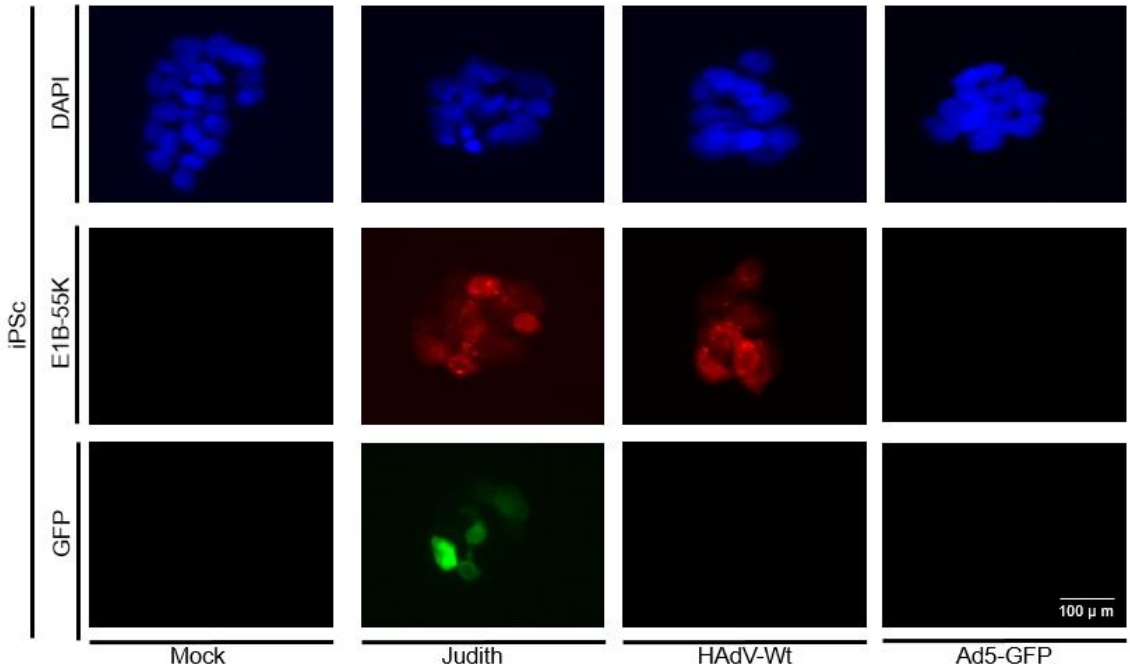

B)

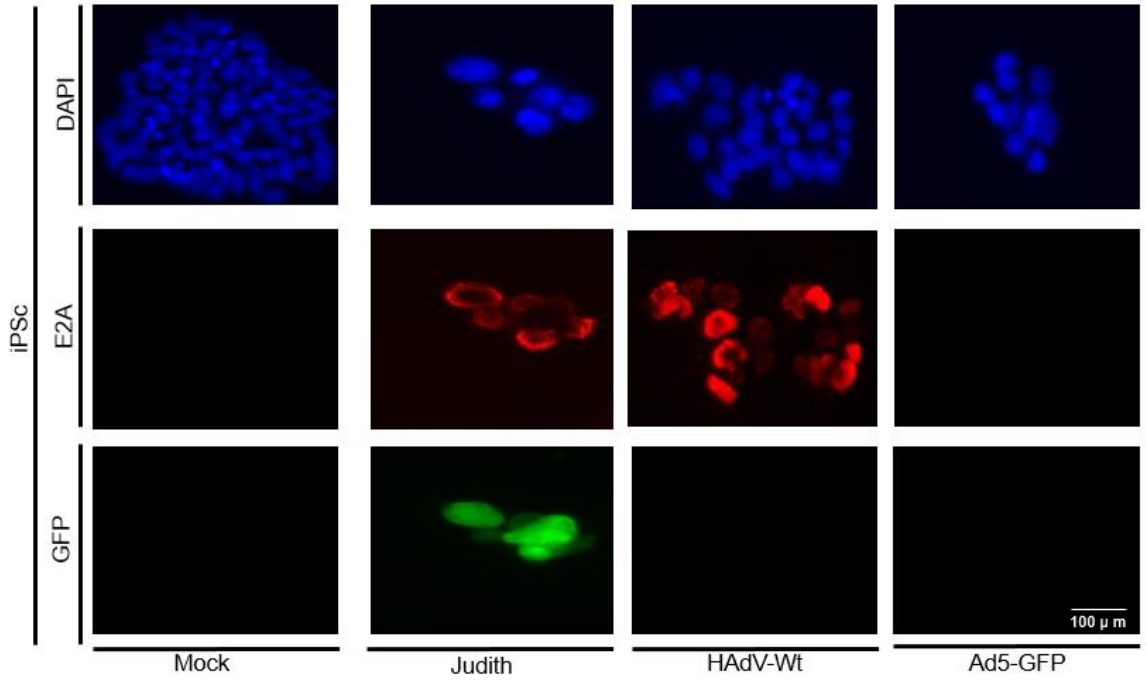

C)

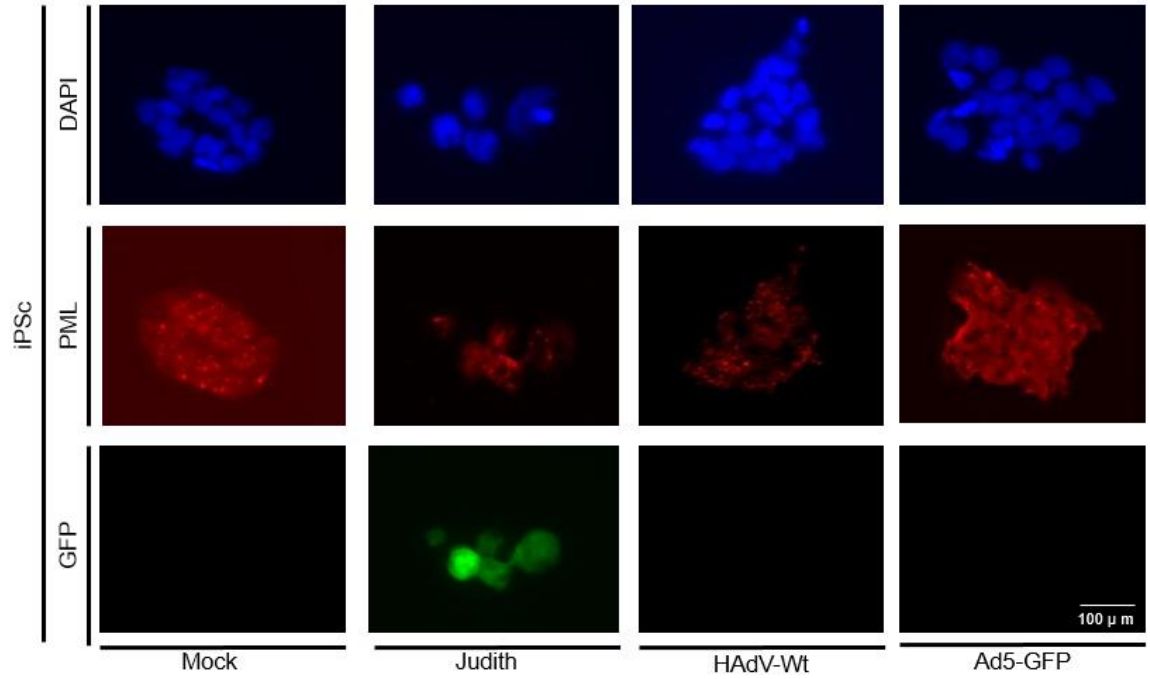

Figure 20: IFA for viral infectivity in iPS cells. A) E1B-55K B) E2A C) PML. iPS cells were infected with three different type of viruses, fixed 72 h p.i. with 4% PFA and double labelled with mAb B6-8 (α-E2A), pAb NB100-59787 (α-PML) and mAb E1B-55K . Primary antibodies were detected using Alexa594 (Red) conjugated secondary antibodies. Imaging was done on Zeiss Axiovert 200M. (Scale bar: 100 µm)

A)

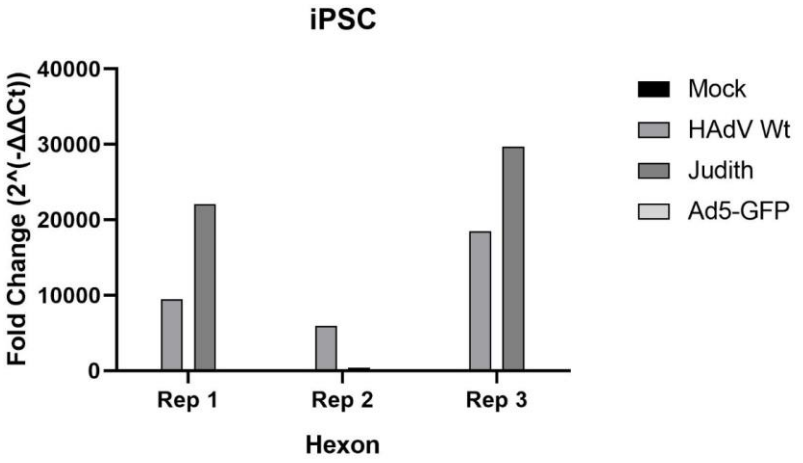
iPSC
Fold Change (2^(-ΔΔCt))
40000
30000
20000
10000
0
Rep 1
Rep 2
Rep 3
Hexon
Mock
HAdV Wt
Judith
Ad5-GFP

B)

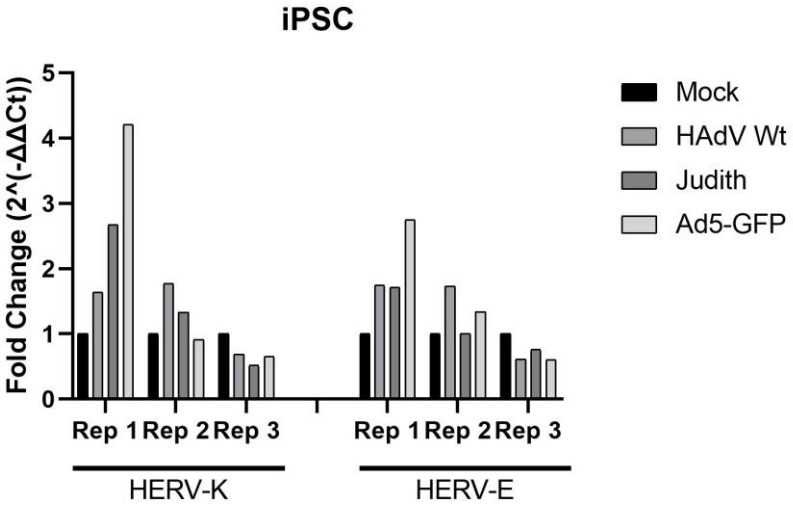
iPSC
Fold Change (2^(-ΔΔCt))
5
4
3
2
1
0
Rep 1
Rep 2
Rep 3
Rep 1
Rep 2
Rep 3
HERV-K
HERV-E
Mock
HAdV Wt
Judith
Ad5-GFP

C)

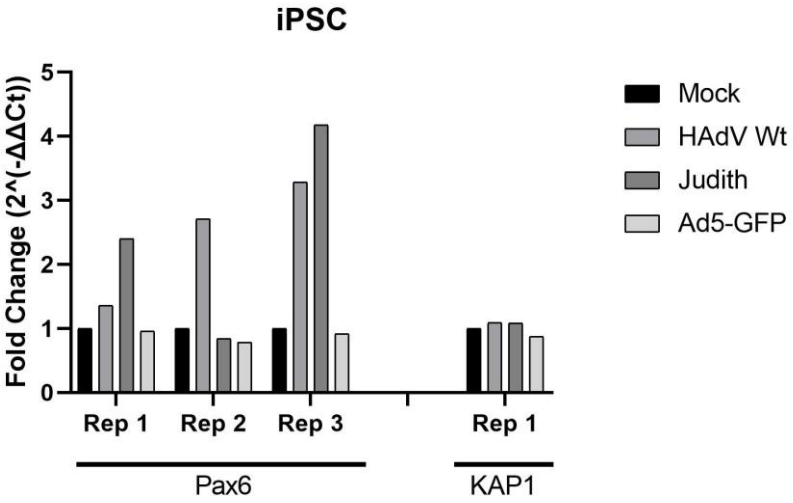
iPSC
Fold Change (2^(-ΔΔCt))
5
4
3
2
1
0
Rep 1
Rep 2
Rep 3
Rep 1
Pax6
KAP1
Mock
HAdV Wt
Judith
Ad5-GFP

D)

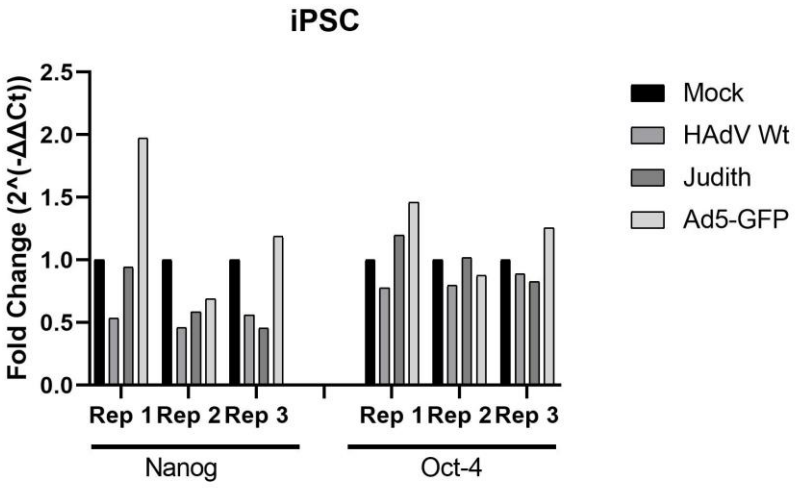

Figure 21: HAdV infection influences HERV families and pluripotency markers in iPSC cells. A) Hexon B) HERV-K, HERV-E C) Pax6, KAP1 D) Nanog, Oct-4. The qRT-PCR study was used to assess the level of mRNA upon infection by HAdV. The graph depicts fold change (2^ (-ΔΔCt)) in mRNA levels normalized to untreated cells. RNA Pol II was served as internal control.

To check the influence of viral infection on pluripotency markers and HERV levels, qRT-PCR was carried out. Hexon levels were measured to take an idea of the amount of virus, and we can see that there is an active infection in Replicate 1 and Replicate 3, but not in Replicate 2 (Fig. 21 A). From qPCR of rep 1, we can see that there is not very much increase in KAP1 levels upon HAdV infection when compared to uninfected control (Fig. 21 C). For HERV-K, there is a significant increase in expression levels in Replicate 1 (~1.5 - 3 folds) upon infection by wt and Judith and rep 2 (~2 folds) upon wt infection, but on the contrary, the expression level of HERV-K decreases in replicate 3 upon infection by both wt and Judith (Fig. 21 B). We investigated HERV-E as it codes for an immunosuppressive env protein (Cherkasova et al. 2016), and stem cells resist infection by ISGs. HERV-E expression increases (~2 folds) in rep 1, 2 upon *wt,* and Judith infection, but decreases expression (~0.5 folds) in infected samples in replicate 3 (Fig. 21 B).

The ability of iPS cells to differentiate into cells of the three germ layers can be functionally defined. Various markers such as Oct-4, Nanog check the pluripotent status of the stem cells (Shi and Jin, 2010). Oct-4 is involved in the preservation of pluripotency. It is highly expressed in pluripotent cells, and its expression decreases upon differentiation (Shi and Jin, 2010). Nanog acts upstream of STAT3 and Oct4 and maintains the clonal expansion of ESC (Chambers et al., 2003). By interacting with other markers, Nanog regulates pluripotency, and cell differentiation (Torres-Padilla and Chambers, 2014). Another factor involved in stem cell pluripotency is Pax6. Pax6

is a regulator of growth with a key function in the central nervous system (CNS), like patterning of the neural tube (Osumi et al., 2008). These markers are highly regulated, and their dysregulation can lead to developmental shortcomings. We monitored three markers Oct-4, Nanog, and Pax6, to test the effect of HAdV infection on the pluripotency dynamics. From the qPCR results, we found that Pax6 levels are increasing (~3 - 4 folds) upon infection by both wt and Judith in replicate 3 (Fig. 21C). In replicate 2, also, we can observe an increase (~3 folds) upon wt infection when compared to mock (Fig. 21 C). There is no substantial change in Oct-4 levels upon HAdV infection for all the replicates (Fig. 21 D), and Nanog levels, on the other hand, decrease (~0.5 folds) upon infection in both wt and Judith infection (Fig. 21 D).

3.2 HAdV infection influences pluripotency markers and HERV levels in standard iPS and KAP1 kd iPS cells

We know that KAP1 is mainly modulated by the early viral E1B- 55K protein and KAP1 is the dominant player involved in the regulation of HERV families. Upon infection, KAP1/SPOC1 complex degrades, which leads to the loss of methylation marks and control of HERVs. To gain more insight into the functionality of KAP1 and to understand the phosphorylation dynamics of KAP1, KAP1 knockdown iPS cell line was generated using lentiviral infection of shRNA targeted to *kap1*. KAP1 knockdown is confirmed with western blotting and qPCR (Fig. 22). As a control for KAP1 knockdown cells, shNeg cells were generated, which had scrambled shRNA not targeted to any gene. Similar to normal iPS cells, shNeg and shKAP1 cells were infected with all three different types of viruses to check the localization of viral proteins IFA studies.

A)

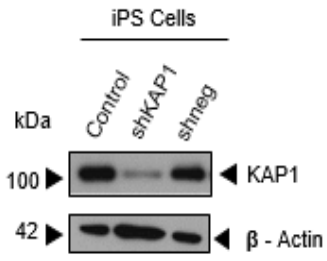

B)

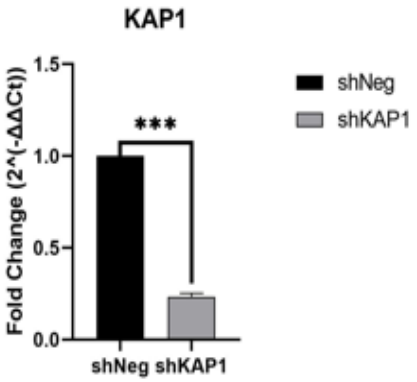

Figure 22: KAP1 knockdown in iPS cells. A) Western Blot B) qRT-PCR. Confirmation of KAP1 knockdown in iPS cells by western blotting and qRT-PCR. Proteins resolved by SDS-PAGE were detected using mouse polyclonal anti-KAP1 and mouse MAb AC-15 (β-actin) as a loading control. To assign the molecular weights of the proteins a protein marker was used. Molecular weights are displayed in kDa on the left side. The graph on the right represents fold change (2^ (-ΔΔCt)) in levels of mRNA normalized to untreated cells. Significance calculated using unpaired t test. (* = p<0.05, ** = p<0.01, ***p < 0.001). Error bars – SEM. RNA Pol II was served as internal control in qRT-PCR.

A)

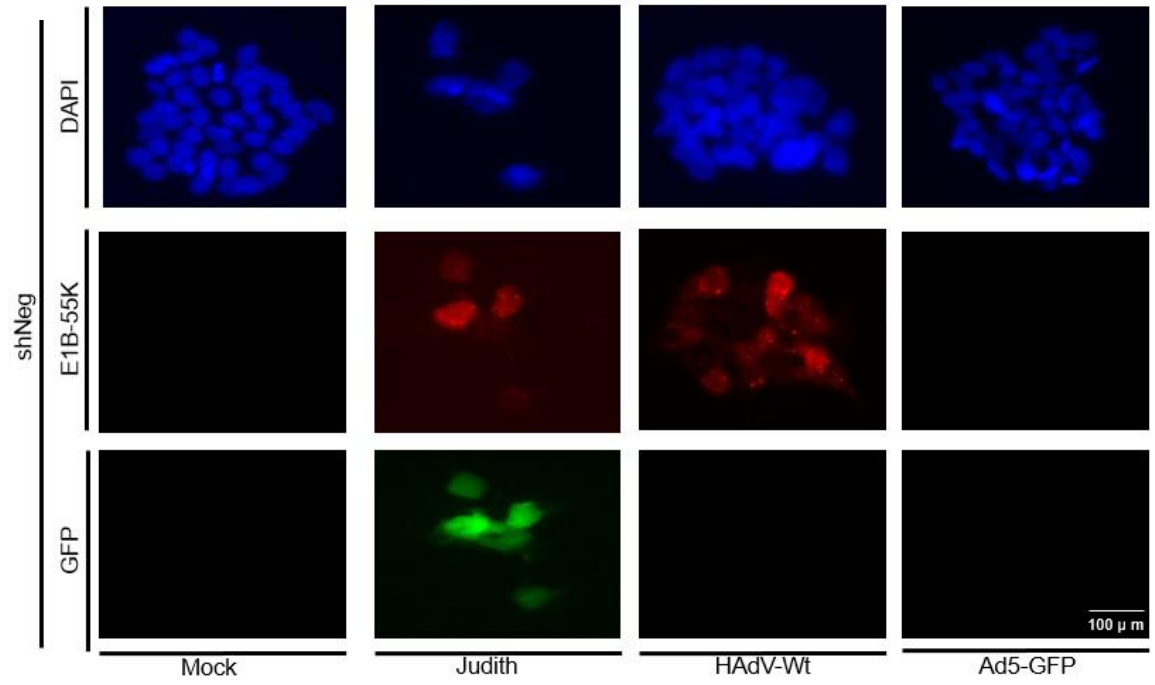

B)

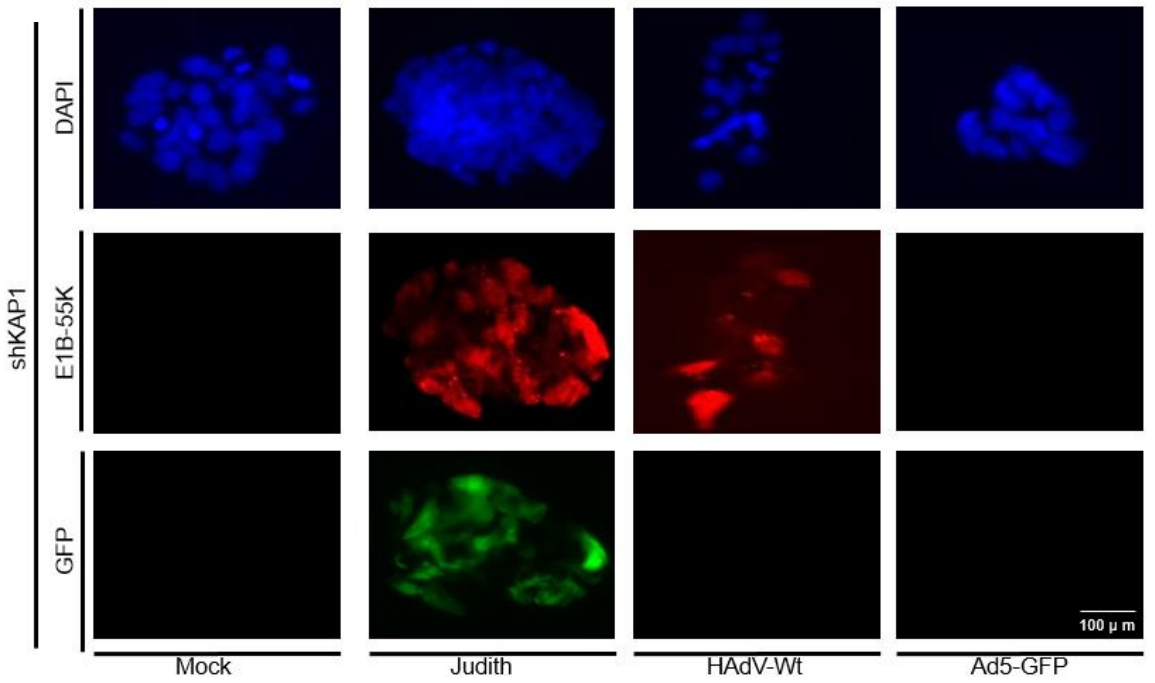

C)

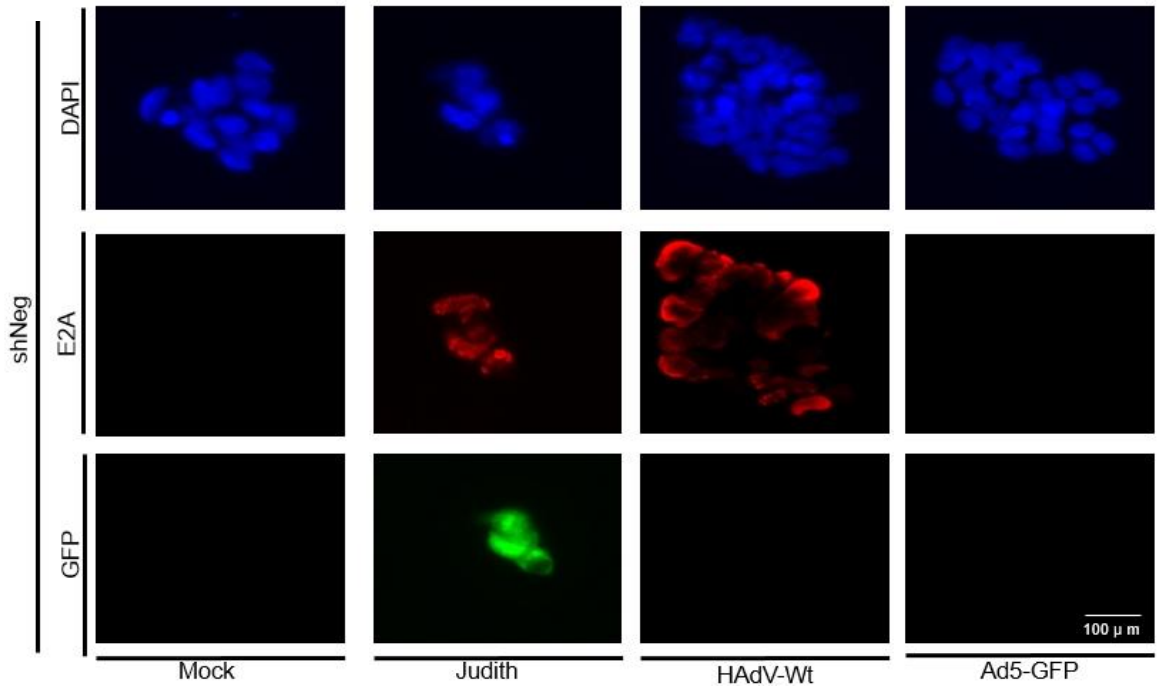
shNeg
DAPI
E2A
GFP
100 µ m
Mock
Judith
HAdV-Wt
Ad5-GFP

D)

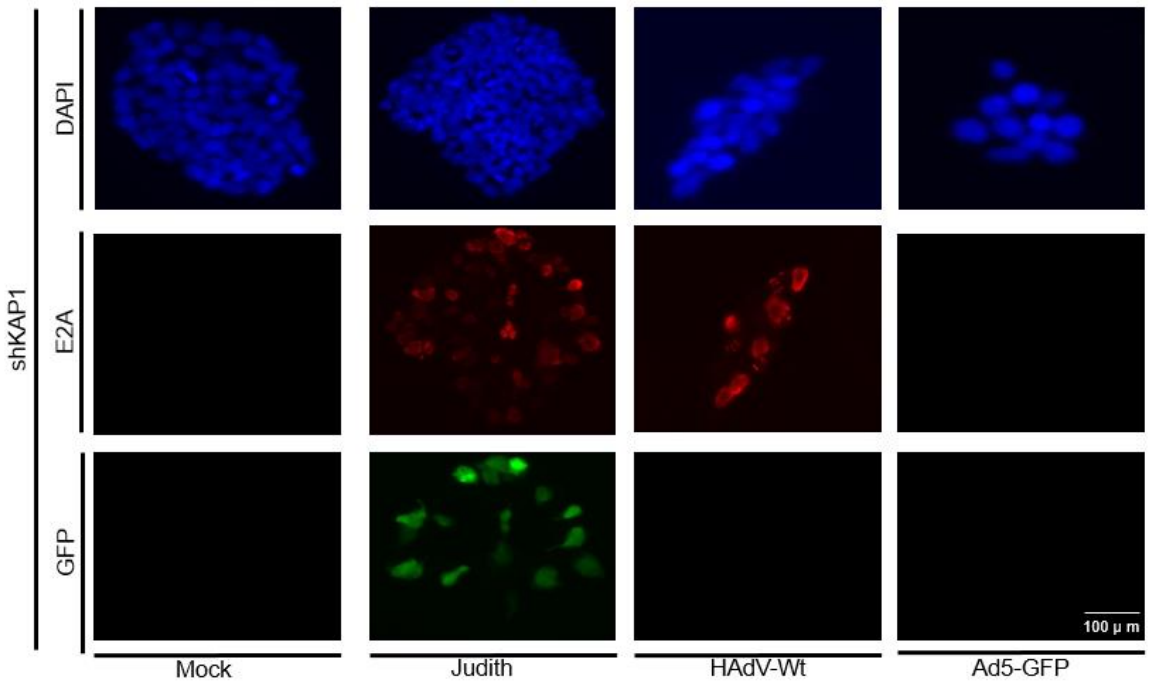
shKAP1
DAPI
E2A
GFP
100 µ m
Mock
Judith
HAdV-Wt
Ad5-GFP

E)

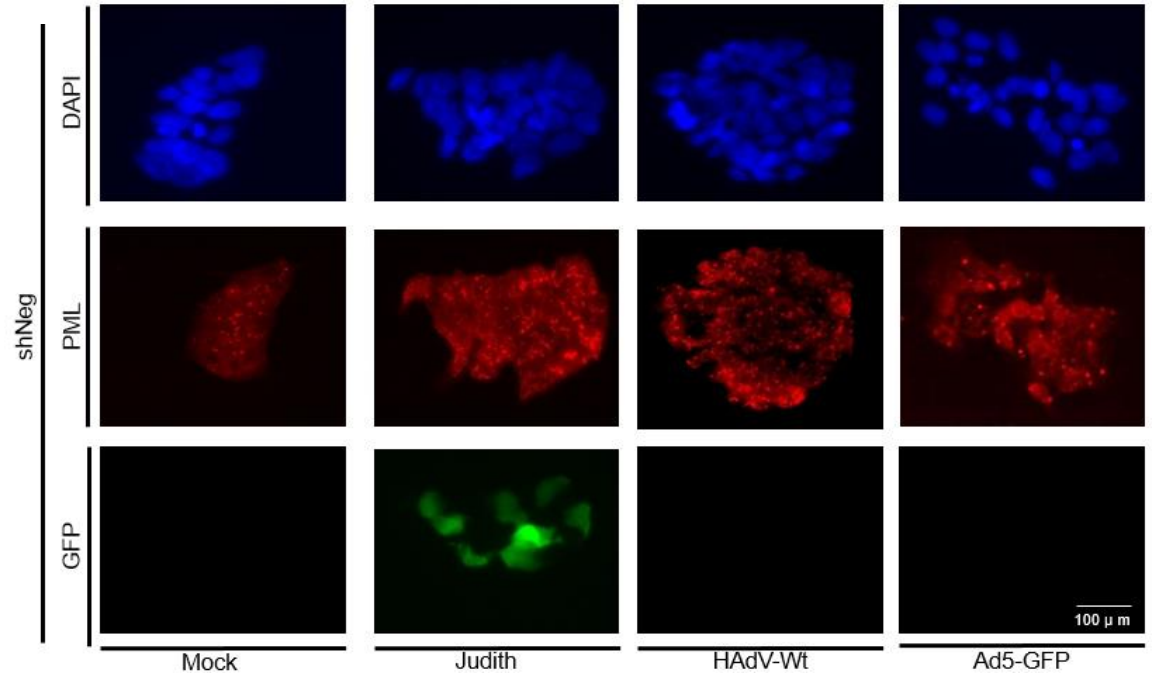

F)

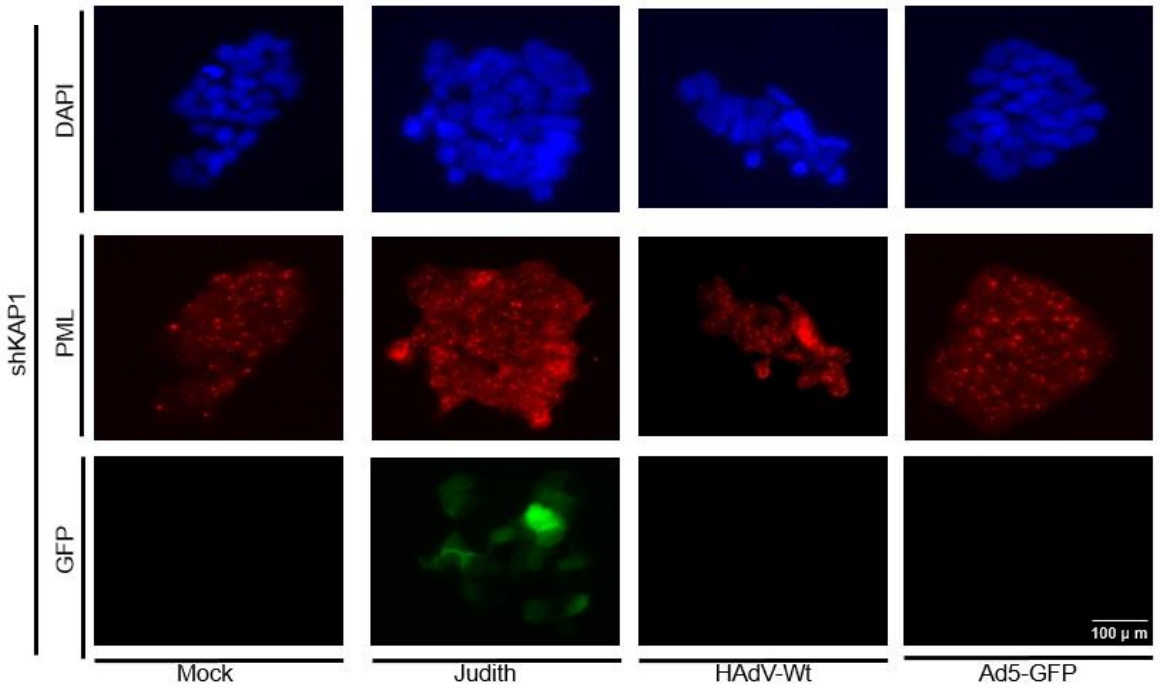

Figure 23: IFA for viral infectivity in shNeg and shKAP1 iPS cells. A) E1B-55K (shNeg) B) E1B-55K (shKAP1) C) E2A (shNeg) D) E2A (shKAP1) E) PML (shNeg) F) PML (shKAP1). shNeg and shKAP1 iPS cells were infected with three different type of viruses, fixed 72 h p.i. with 4% PFA and double labelled with mAb B6-8 (α-E2A), pAb NB100-59787 (α-PML) and mAb E1B-55K . Primary antibodies were detected using Alexa594 (Red) conjugated secondary antibodies. Imaging was done on Zeiss Axiovert 200M. (Scale bar: 100

From the IFA studies, we can see that there is not much change in the localization of viral proteins or PML upon KAP1 knockdown. E2A staining pattern in shNeg (Fig. 23 B) and shKAP1 (Fig. 23 C) cell line is similar to normal iPS cells (Fig. 20 B) representing the viral replication centers. We know that E4orf3 protein reorganizes PML-NBs into track-like structures (Doucas et al. 1996), and these structures can be observed in the infected shNeg (Fig. 23 C) and shKAP1 (Fig. 23 F) similar to what we see in normal iPS cells (Fig. 20 C). In adenovirus-infected cells, most of the E1B-55K protein localizes in the nucleus or near the nucleus, and we can observe in infected cells, the localization of E1B-55K is mainly nuclear in both shNeg (Fig. 23 A) and shKAP1 cells (Fig. 23 D). The localization patterns of E1B-55K, E2A, and PML in shNeg and shKAP1 cells look similar to what we observe in normal iPS cells (Fig. 20).

To determine how pluripotency markers and HERVs are modulated upon KAP1 knockdown, we infected the iPS, shNeg, and shKAP1 with different HAdV viruses. Western blot was done to check KAP1 modulation, and qRT-PCR was done for pluripotency markers and HERV levels.

A)

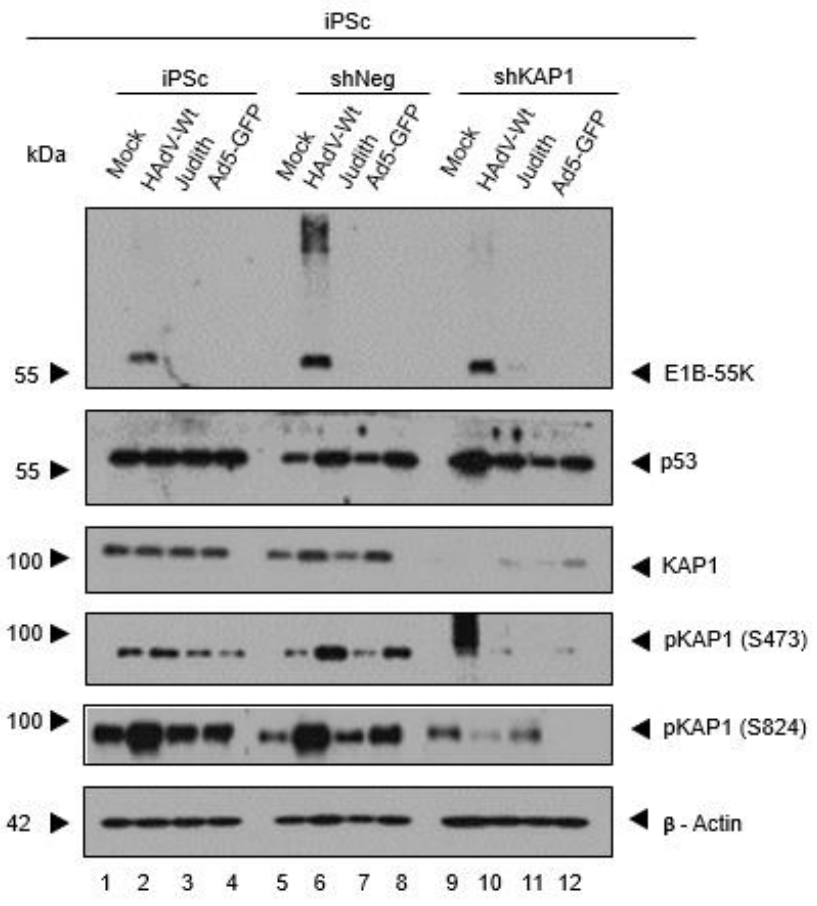

B)

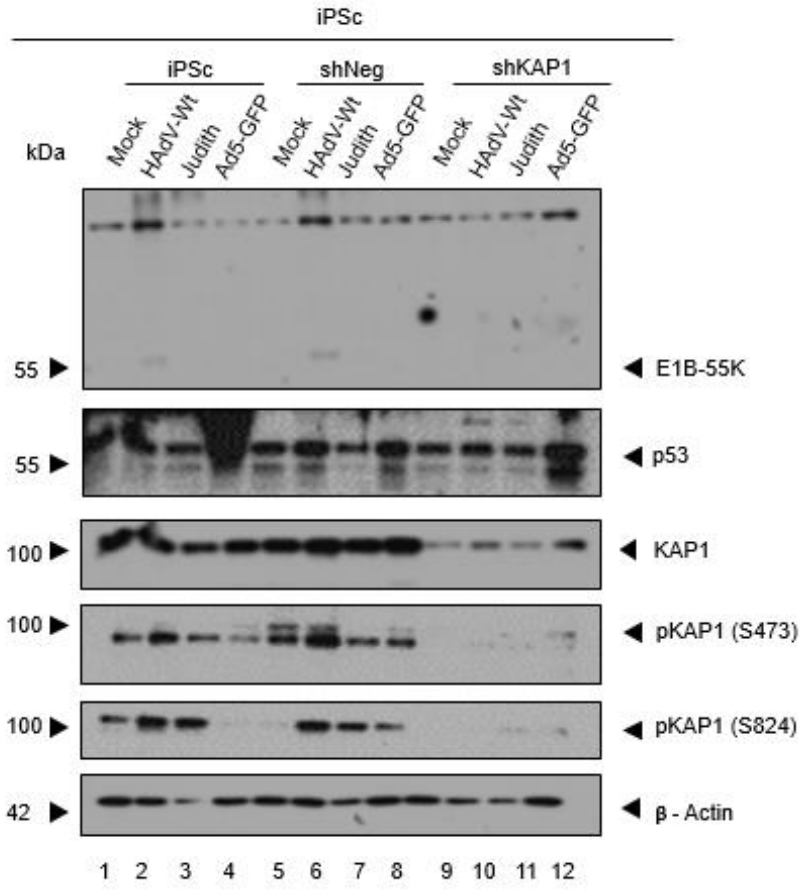

Figure 24: HAdV infection influences KAP1 PTMs in iPS, shNeg and shKAP1 cell line. A) Replicate II B) Replicate III. Cells from respective cell lines were seeded and infected with all three different types of HAdV. Proteins resolved by SDS-PAGE were detected using mouse MAb 2A6 (anti-E1B-55K), mouse polyclonal anti-KAP1, rabbit polyclonal Ab pKAP1S473, rabbit polyclonal pKAP1S824, rabbit polyclonal anti-p53 and mouse MAb AC-15 (β-actin) as a loading control. To assign the molecular weights of the proteins a protein marker was used. Molecular weights are displayed in kDa on the left side.

From the western blots, we can see that there is no streak in E1B-55K stain representing the high SUMOylation of protein. Instead, we observe just a single band (Fig. 24 A). Contrary to A549 (Fig. 7) and HepaRG (Fig. 11), there is no SUMOylation and degradation of p53 upon infection in standard iPS, shNeg, and shKAP1 cells. KAP1 knockdown can be confirmed in both the replicates (Fig. 24 lanes 9, 10, 11, and 12) by the absence of the KAP1 band. We can also see that in standard iPS and shNeg cells, KAP1 degradation is not very high in infected samples (lane 2, 3, 4, 6, 7, and 8) compared to uninfected mock (lane 1 and 5). Similar to other cell lines like A549 (Fig. 7), there is an increase in pKAP1 (S824) levels upon HAdV-*wt* infection in standard iPS (Fig. 24 lane 2) and shNeg cells (Fig. 24 lane 6) when compared to uninfected mock. There are no observable change in pKAP1 (S473) levels upon infection.

A)

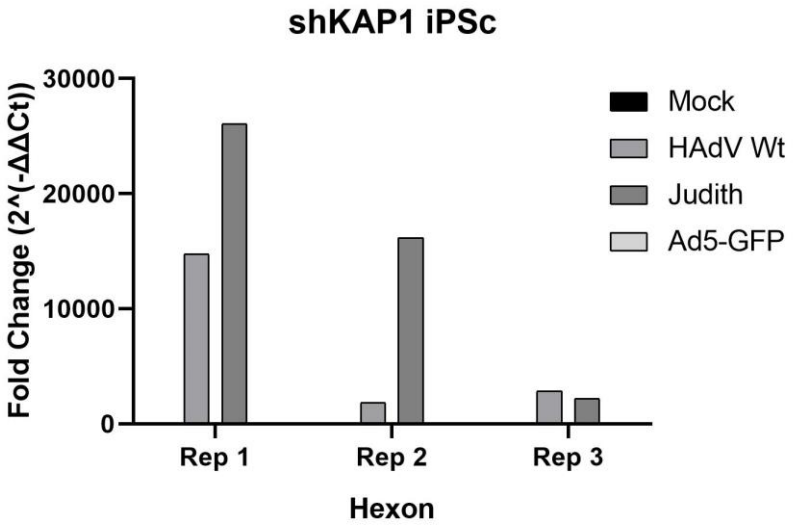
shKAP1 iPSc
Fold Change (2^(-ΔΔCt))
30000
20000
10000
0
Rep 1
Rep 2
Rep 3
Hexon
Mock
HAdV Wt
Judith
Ad5-GFP

B)

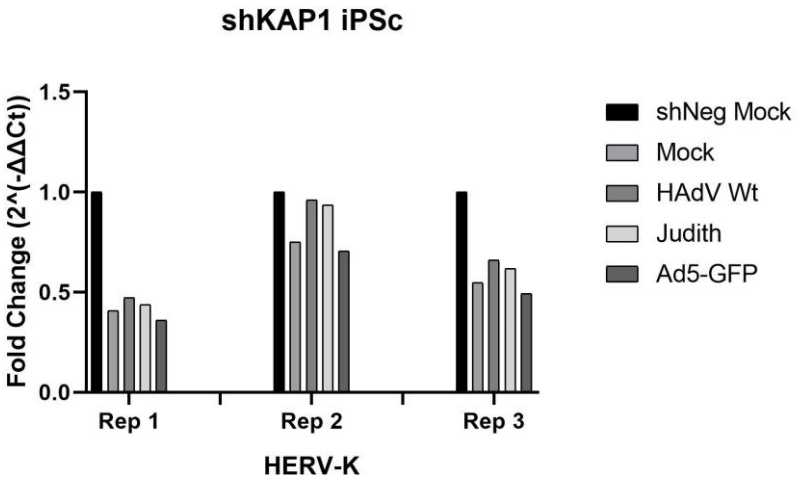
shKAP1 iPSc
Fold Change (2^(-ΔΔCt))
1.5
1.0
0.5
0.0
Rep 1
Rep 2
Rep 3
HERV-K
shNeg Mock
Mock
HAdV Wt
Judith
Ad5-GFP

C)

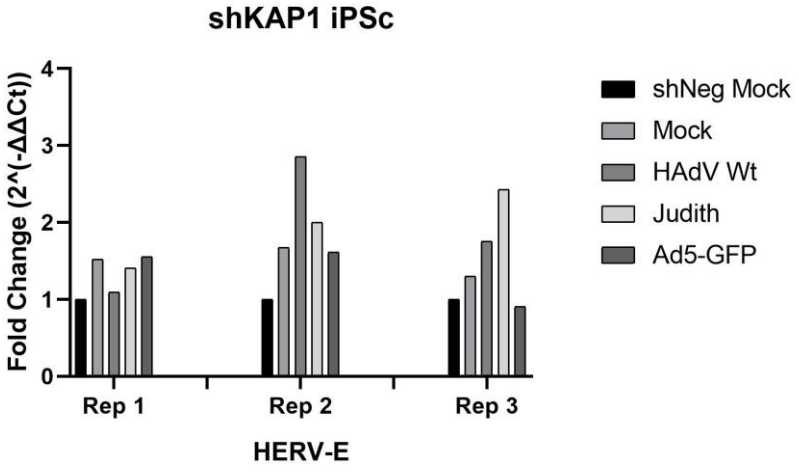
shKAP1 iPSc
Fold Change (2^(-ΔΔCt))
4
3
2
1
0
Rep 1
Rep 2
Rep 3
HERV-E
shNeg Mock
Mock
HAdV Wt
Judith
Ad5-GFP

D)

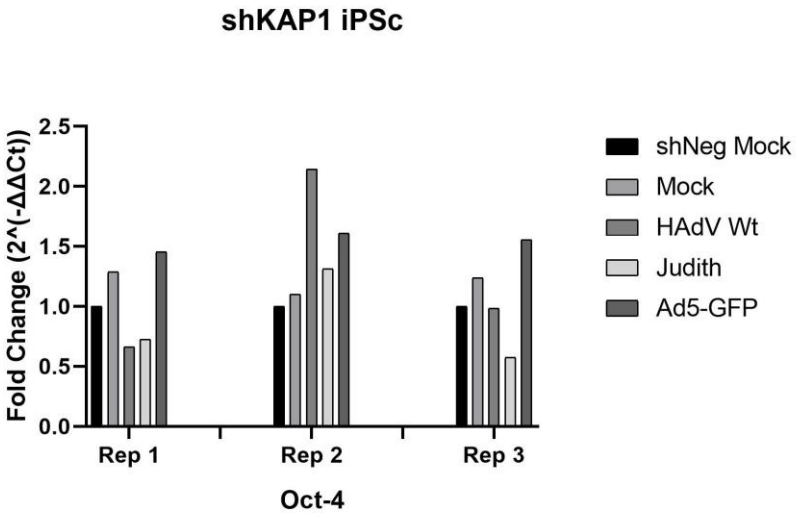

E)

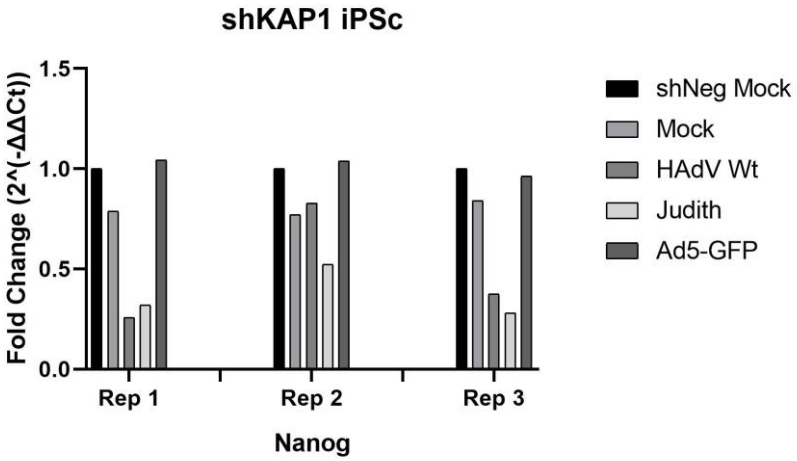

F)

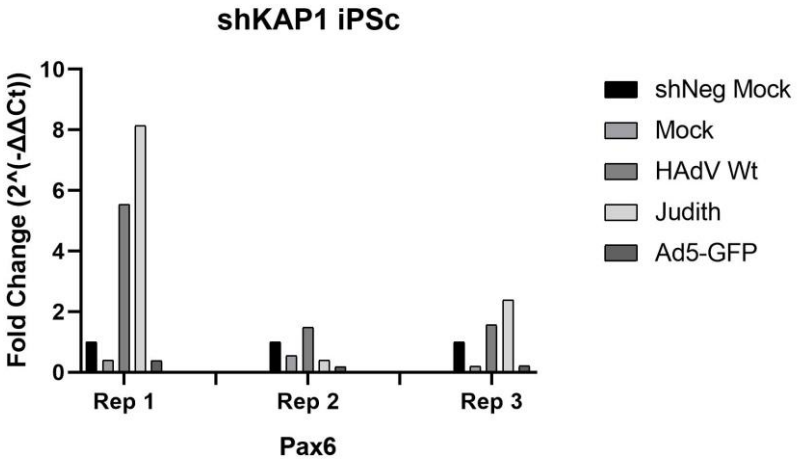

Figure 25: HAdV infection changes HERV and pluripotency marker levels in shKAP1 iPS cells. A) Hexon B) HERV-K C) HERV-E D) Oct-4 E) Nanog F) Pax6. The qRT-PCR study was used to assess the level of mRNA upon infection by HAdV. The graph depicts fold change (2^ (-ΔΔCt)) in mRNA levels normalized to shNeg untreated cells. RNA Pol II was served as internal control.

From the qRT-PCR graphs, we can see Hexon levels in all replicates representing the infection by HAdV-*wt* and Judith. Still, in replicate 3, the amount of Hexon is less (~ 3000 folds) compared to uninfected mock whereas in rep 1 and 2 hexon expression is very high (~15000 – 25000 folds) (Fig. 25 A). There is no observable infection for the Ad5-GFP variant. To check influence on HERV elements, HERV-K and HERV-E are analyzed as both of them are modulated by KAP1. We can see that upon KAP1 knockdown, HERV-K level decreases (~0.4 folds) in both wt and Judith infection in rep 1, whereas in rep 3, the reduction is ~0.6 folds in infected samples compared to uninfected mock of shNeg (Fig. 25 B). Upon infection by HAdV-*wt* and Judith, HERV-E expression increases (~1.8 – 2.8 folds) compared to uninfected shNeg control (Fig. 25 C). To check the effect of KAP1 knockdown and HAdV infection on pluripotency in iPS cells, three pluripotency markers were monitored. Upon knockdown, we can see that Pax6 (~0.3 folds) and Nanog (~0.8 folds) decreases, and there is little increase in Oct-4 levels (~1.2 folds). However, upon infection by wt and Judith, we can observe that there is an increase in Pax6 levels (~4 folds), whereas Nanog levels (~0.4 folds) decreases upon infection (Fig. 25 E, F). We can see an increase in Oct-4 levels upon infection in replicate two (~2 folds), but in other replicates, there is not much change in Oct-4 levels (Fig. 25 D).

From the qPCR results, we found that the Pax6 level increases upon both HAdV-*wt* and Judith infection (Fig. 25 E). To check its localization, we performed the IFA for different viral proteins and Pax6. *Pml*$^{-/-}$ iPSC expresses higher levels of Pax6 (Hadjimichael et al. 2017). We also know that E4orf3 viral protein is involved in the track-like formation of PML bodies and inhibits their function (Doucas et al. 1996; Stubbe et al., 2020). E2A is a marker for viral replication centers. From the IFA images, we can see that E2A staining is dot-like representing replication centers within the nucleus (Fig. 26 A, C, and E), and E4orf3 staining is mostly nuclear (Fig. 26 B, D, and F). Pax6 staining is mainly and can be seen in all cells but more concentrated in infected cells (Fig. 26).

A)

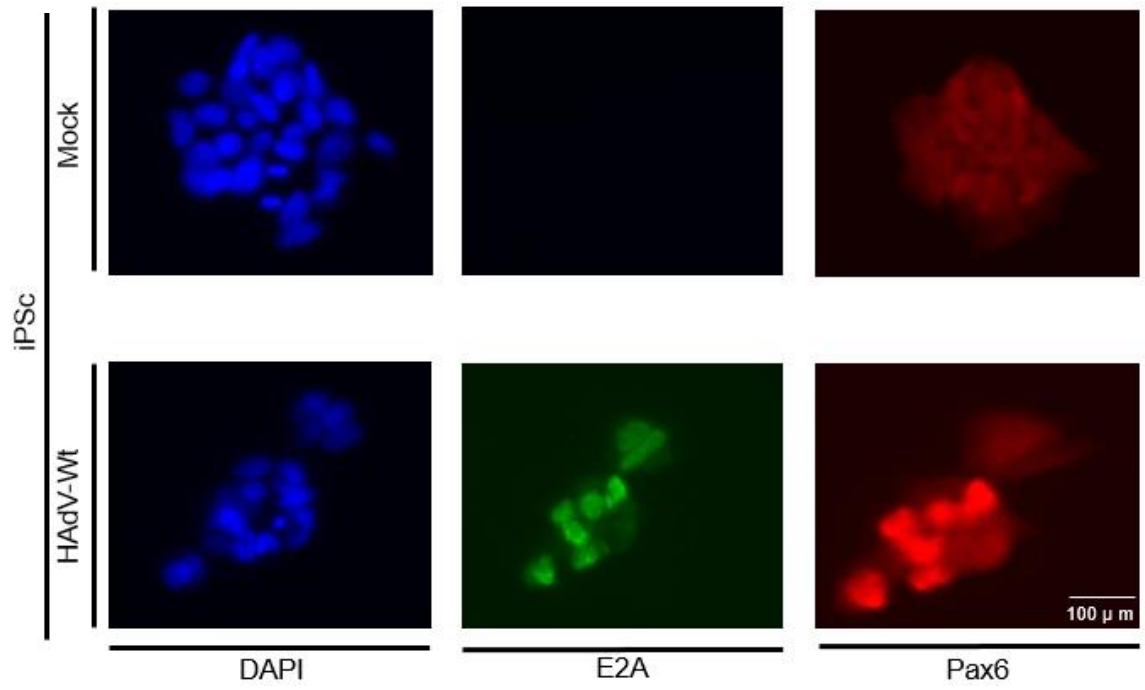
iPSc
Mock
HAdV-Wt
100 µ m
DAPI
E2A
Pax6

B)

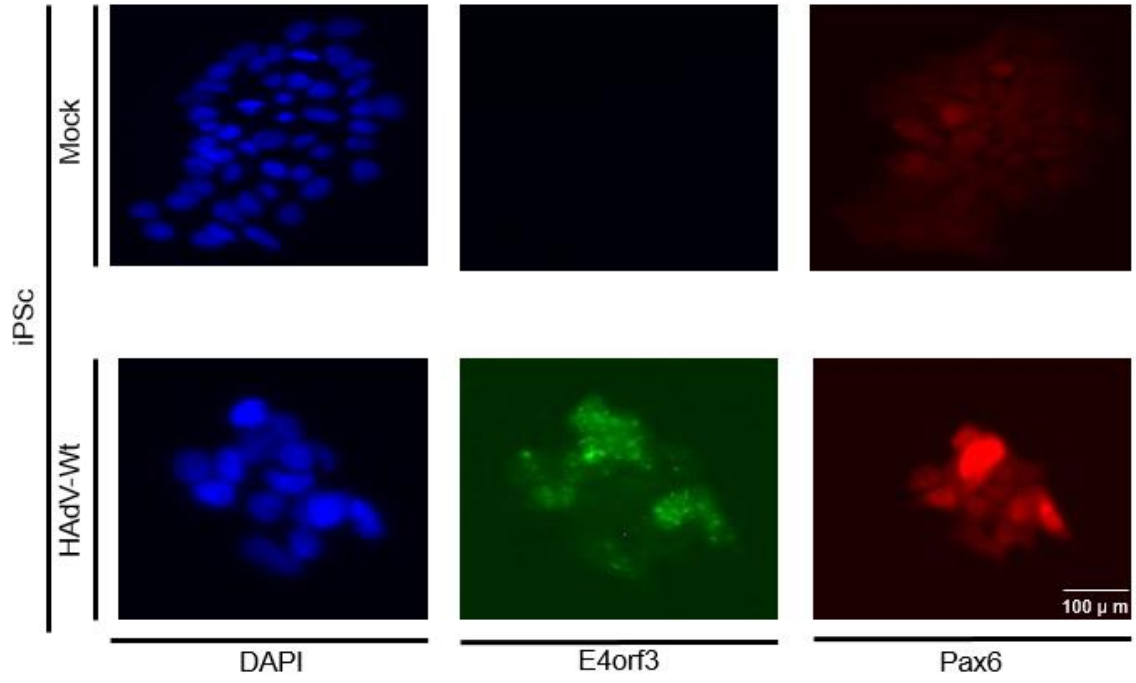
iPSc
Mock
HAdV-Wt
100 µ m
DAPI
E4orf3
Pax6

C)

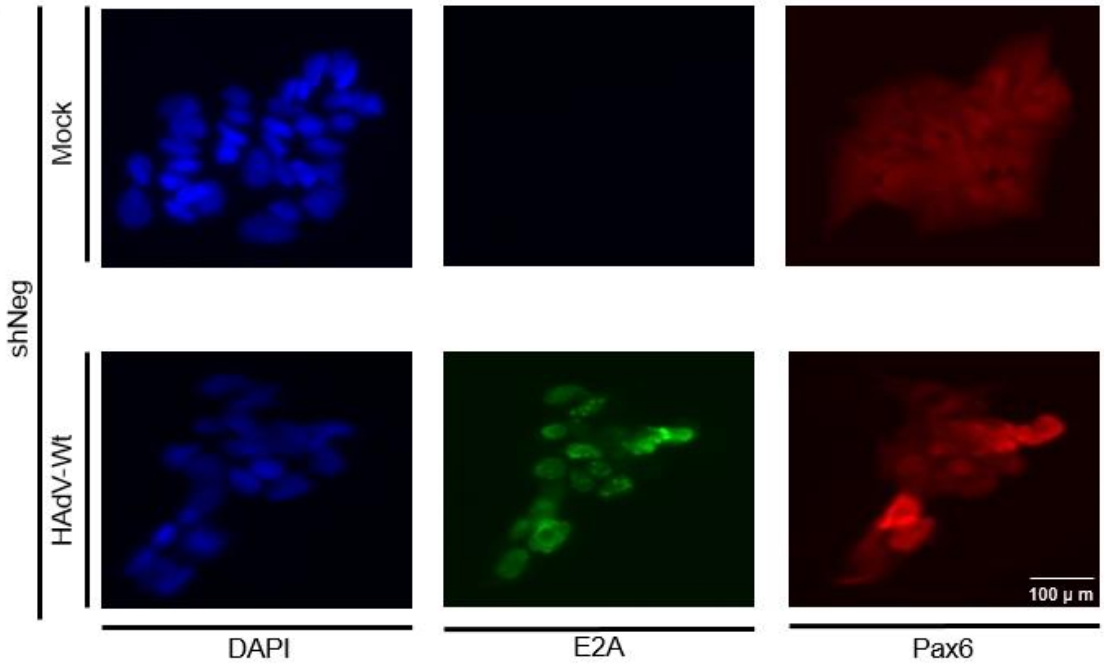
shNeg
Mock
HAdV-Wt
100 µ m
DAPI
E2A
Pax6

D)

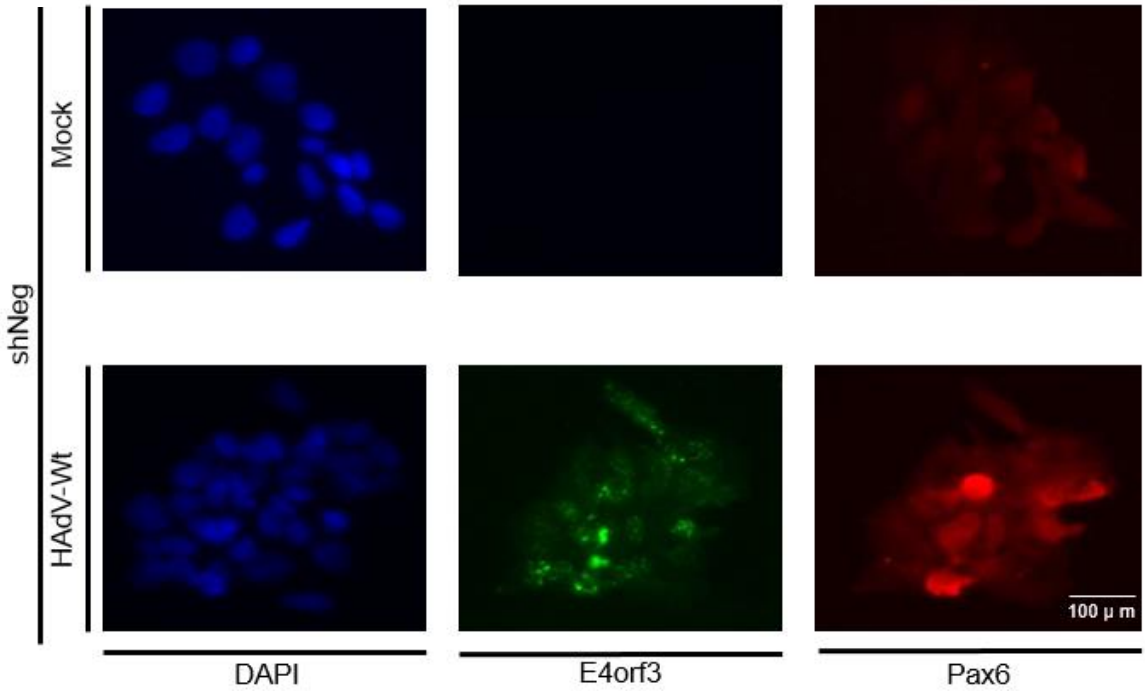
shNeg
Mock
HAdV-Wt
100 µ m
DAPI
E4orf3
Pax6

E)

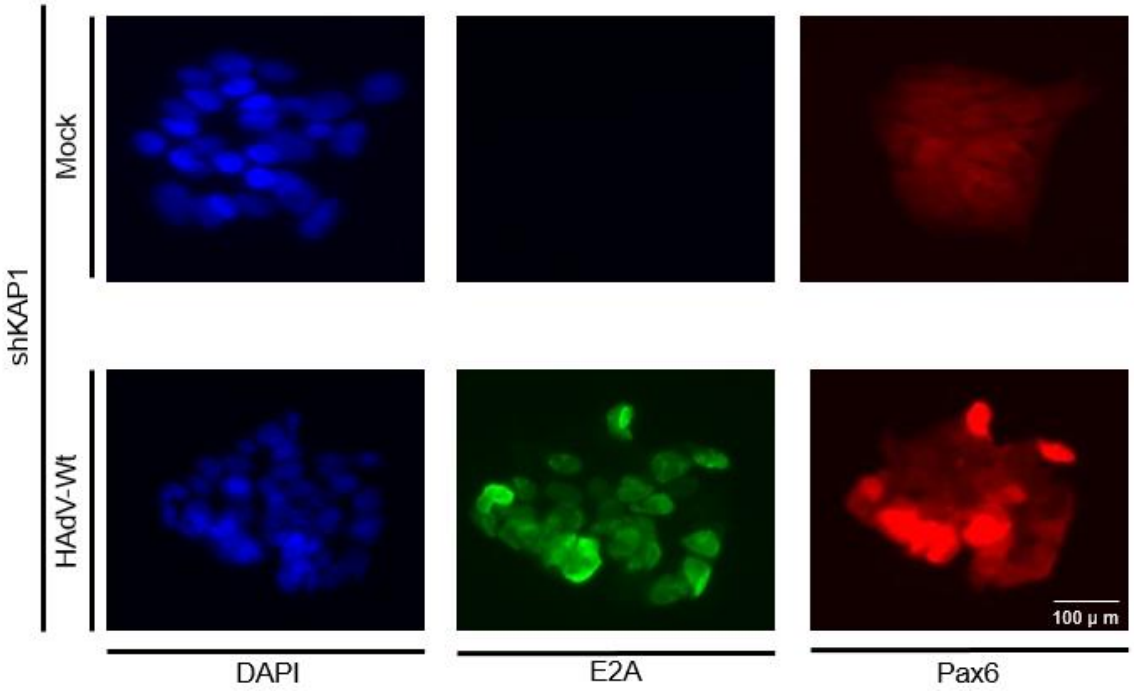

F)

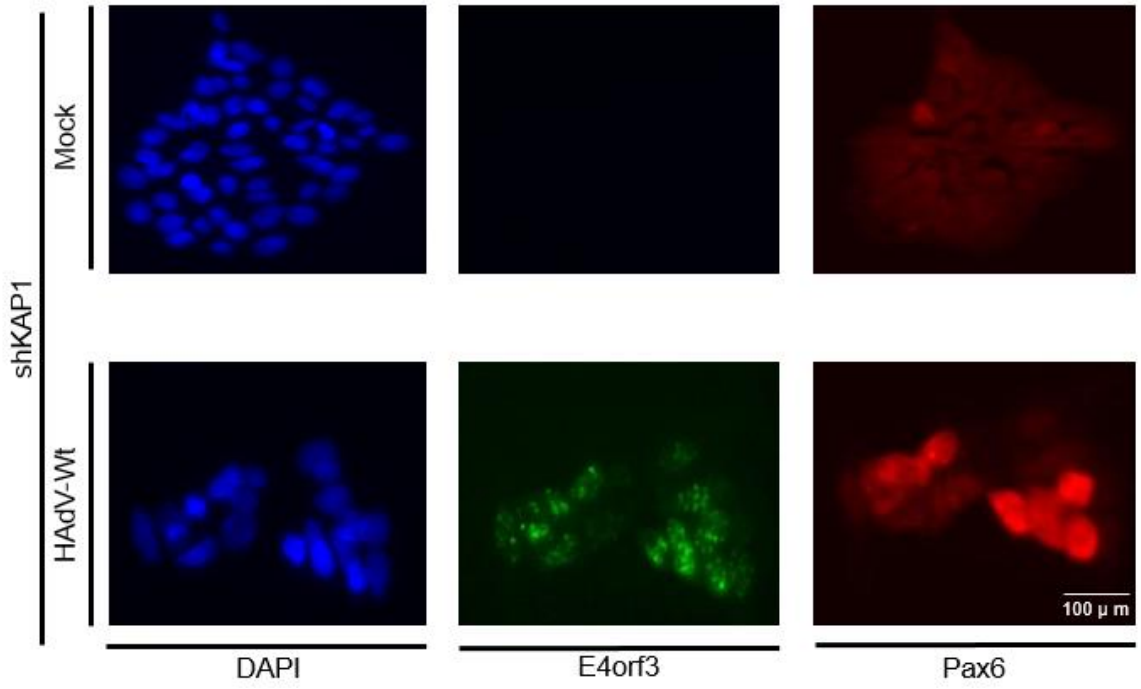

Figure 26: IFA for viral protein and Pax6 in shNeg and shKAP1 cells upon HAdV - *wt* infection. A) E2A + Pax6 (iPSc) B) E4orf3 + Pax6 (iPSc) C) E2A + Pax6 (shNeg) D) E4orf3 + Pax6 (shNeg) E) E2A + Pax6 (shKAP1) F) E4orf3 + Pax6 (shKAP1). IPSc, shNeg and shKAP1 cells were infected with HAdV - *wt*, fixed 72 h p.i. with 4% PFA and labelled with mAb B6-8 (α-E2A), mAb 6A-11 (α-E4orf3), and rabbit Pax6. Primary antibodies were detected using Alexa594 (Red) and Alexa488 (Green) conjugated secondary antibodies. Imaging was done on Zeiss Axiovert 200M. (Scale bar: 100 µm)

DISCUSSION

KAP1 is an evolutionarily conserved protein that is involved in transcriptional repression and controls its functionality via crosstalk between its PTMs like SUMOylation and phosphorylation. SUMOylated KAP1 represents the original state of KAP1 in the cell and is involved transcriptional silencing (Iyengar and Farnham 2011; Bürck et al. 2016).

KAP1 can get phosphorylated at various positions, with each of them involved in different functions. DDR triggers ATM and induces phosphorylation of serine at position 824, making the KAP1 functionally inactive (Iyengar and Farnham 2011; Bürck et al. 2016). Another important phosphorylation site is Serine 473. Phosphorylation of Serine 473 is vital in cell cycle regulation. This phosphorylation and *cyclin A2* gene get induced at the same time during the cell cycle. It also regulates Heterochromatin Protein 1 (HP1) binding and corepressor function (Chang et al., 2008). HAdV alters KAP1 PTMs for efficient viral replication. E1B-55K protein gets SUMOylated by the SUMOylated KAP1, and in turn, SUMOylated E1B-55K phosphorylates the KAP1 at site 824. This leads to dissociation of the KAP1 repressive complex resulting in transcriptional activation and enhanced adenoviral gene expression (Bürck et al. 2016).

Besides this, KAP1 is the principal epigenetic restriction factor, which represses human endogenous retroviruses (HERVs) in human cells (Rowe et al., 2010). It was shown that HAdV combats the repressive function of KAP1 (Bürck et al., 2016). Additionally, KAP1 knockdown leads to the removal of repressive marks placed on retroelements (Turelli et al., 2014). Current knowledge implies that specific pathologies, including cancer, are associated with the expression of HERVs. In this project, we investigated the influence of HAdV infection on the PTMs of KAP1 and, in turn, to consider the modulation of different HERVs.

In this research project, we investigated the influence of HAdV infection on the PTM status of KAP1 and HERV regulation in several human cancer cell lines. HepaRG cell line is different from other cell lines like A549, H1299 as HepaRG is of hepatic origin, whereas A549 and H1299 are lung cells, and HAdV infection progresses differently in HepaRG cells. In HepaRG, infection is delayed, and E1B-55K protein forms

cytoplasmic aggregates. It gets localized in globular condensations, which lie near the E2A containing ring-like structures (Schreiner et al., 2010). A549 and H1299 cells are both epithelial, whereas HepaRG cells are terminally differentiated hepatic cells. They originate from a progenitor cell line, which has several properties of primary human hepatocytes (Marion et al. 2010). Several studies suggest that pKAP1 (S473) is also involved in the immune response. It has been shown that Kaposi's Sarcoma-Associated Herpesvirus (KSHV) infection induces KAP1 phosphorylation at serine-473 in endothelial cells (King 2013). Due to the different architecture of cell lines, it is possible that upon adenoviral infection in HepaRG, pKAP1 (S473) increases in response to immune signals. To examine the potential reactivation of HERVs in adenoviral infection, qRT-PCR was done. We could not observe significant changes in HERV-H levels upon infection in all three cell lines, which was expected as KAP1 does not regulate it. HERV-H shows the level of stemness of the cells and is expressed in minimal quantities in differentiated cells and is aligned with H3K4me3 marks (Santoni et al. 2012). Low HERV levels might be due to the RNA degradation of HERVs at the level of post-transcription or RNA interference (Gupta et al., 2014). In HepaRG, we could not observe any significant change in HERV levels (Fig. 12). It might be possible due to the dynamics of pKAP1 (S473) or tissue-specific expression of HERVs. It has also been reported that there is a deficient expression of HERVs in hepatic cells (Seifarth et al. 2005), so it is possible that because of this and different phosphorylation dynamics of KAP1 Ser473, no change was observed in HERVs. To gain more insight, cell lines of varying origin expressing KAP1 mutated at different serine positions should be used. Furthermore, we should monitor other PTMs also.

We know that adenoviral protein E1B-55K mainly modulates KAP1 PTMs that leads to disruption of KAP1 repressive complex, which might lead to HERV upregulation. To check which other adenoviral protein is involved in the HERV regulation, we tested already generated HAdV variants with depletions in various regulating viral genes to gain novel insight into the molecular background of HERV modulation during infection. From the western blots, we can observe that in the absence of E1B-55K and E4orf6 protein, there is no degradation of KAP1 and p53 (Fig. 13, 15, and 17) as E4orf6 and E1B55K proteins were shown to interact during infection (Sarnow et al., 1982) and to function in the same pathway. E1B-55K/E4orf6 expression after HAdV infection leads to degradation of the KAP1/SPOC1 complex, followed by a reduction of H3K9me3

repressive histone marks (Schreiner et al., 2013). We found that upon infection by different HAdV variants, HERV-K level decreases in A549 (Fig. 14), suggesting there might be a different protein involved in its regulation like APOBEC3G. Human apolipoprotein B mRNA-editing complex 3 (APOBEC3G) inhibits reverse transcription of the proviral genome, and disruption of APOBEC3G can lead to enhanced expression of HERV elements (Okada and Iwatani 2016). It has also been reported that the *vif* gene of HIV1 hampers the activity of APOBEC3G (Stopak et al. 2003). Some adenoviral protein may obstruct the APOBEC3G functioning leading to HERV upregulation. To check this hypothesis, we can use the shAPOBEC3G cell line, and we can look for any other interaction partner of APOBEC3G via Co-IP. As we know that HERV expression and adenoviral infection is tissue-specific and in hepatic cells, the expression of HERV is very less (Seifarth et al. 2005), so it possible that in HepaRG cells, there are multiple proteins involved in the regulation of HERVs not only KAP1 (Fig. 18). E1B-55K and E4orf6 together modulate KAP1, which in turn modulates the HERV expression. It has also been reported that *np9* interacts with RING-type E3 ubiquitin ligase LNX and promotes tumorigenesis (Armbruester et al. 2004). E3 ubiquitin ligase formed by E1B-55K/E4orf6 may contribute to the observed increase in HER-W and HERV-T levels in H1299 cells (Fig. 16). Increased expression of HERV elements is found to be associated with many defects like high levels of HERV-W are found in cancer, multiple sclerosis samples. Adenovirus is also detected in different cancers tissue. So, it is crucial to investigate the link between adenovirus and HERVs.

KAP1 controls HERVs in early embryonic development (Rowe et al., 2010). It has also proved to be an essential determinants of the reprogramming process of human-induced pluripotent stem cells (hiPSCs) (Balestrieri et al., 2018). hiPSCs have distinct genomic architecture as compared to cancer cells. Their chromatin is much more relaxed and accessible for proteins, and HERV expression is also different than cancer cell lines. Due to the expression of interferon stimulating genes (ISGs), stem cells are immune to infections (Haas and Trumpp, 2018). So we expect different modulation of KAP1 and HERV in iPSCs upon HAdV infection.

Furthermore, in our study, to gain more insight into modulation by KAP1, we generated KAP1 knockdown iPS cell line. *Kap1* deletion in ESC leads to loss of pluripotency, failure to silence endogenous, or exogenous retroviruses (Rowe et al., 2010). We

infected normal, shNeg, and shKAP1 iPS cells with different types of HAdV-*wt,* Judith, and replication-incompetent Ad5-GFP. From the western blot, we observed the absence of streak in the E1B-55K blot and SUMOylation of p53 (Fig. 24). We did not see the degradation of KAP1 also (Fig. 24), which might be due to the different SUMOylation pathway in iPS cells. SUMO functions in ESCs by stabilizing H3K9me3 heterochromatin genome-wide and KAP1-HP1α are involved in SUMO-dependent maintenance of H3K9me3 levels (Cossec et al., 2018). If the E1B-55K protein is not SUMOylated, then it cannot SUMOylates and degrades KAP1, which in turn, modulates HERVs. qRT-PCR was done to highlight the changes in HERV elements and pluripotency markers. We found an increase in HERV-K levels in normal iPS cells (Fig. 21), but a decrease in KAP1 knockdown iPS cells (Fig. 25) upon infection. The reduction in HERV expression might be due to the post-transcriptional HERV RNA degradation (Gupta et al., 2014). Recent studies highlight that HERVs are repressed via DNA methylation, RNA degradation, or in some cases, RNA interference (Gupta et al., 2014). It is possible that upon adenoviral infection, retroviral RNA is degraded via RNA interference. Also, the KAP1 knockdown achieved in this study is around 80%, so for a clear understanding, KAP1 knockout cell lines can be used in further experiments.

KAP1 also plays a vital role in preserving the pluripotency of stem cells. It makes a complex with Oct4 and maintains an undifferentiated state of stem cells in a phosphorylation-dependent manner (Seki et al. 2010). Oct-4, together with Sox2, regulates Nanog and maintains ESC pluripotency (Silva et al., 2009; Young, 2011). So, the disruption of KAP1 will also influence stem cell pluripotency. It is previously reported that KAP1 knockdown in stem cells leads to a decrease in Nanog and Oct-4 levels (Oleksiewicz et al. 2017). In our experiments also, a reduction in Nanog levels was observed (Fig. 25) but not in Oct-4 levels upon KAP1 knockdown. It is possible that knockdown was not enough to affect the levels of Oct-4. We also observed a decrease in Pax6 levels in KAP1 knockdown cells (Fig. 25). Pax6 is also known to interact with KAP1 (Pavlaki et al. 2018). We know that KAP1 influences pluripotency markers. Upon adenoviral infection, KAP1 dynamics are changed, so to investigate the effect of adenoviral infection on pluripotency, we infected the normal and shKAP1 iPS cells. We observed no change in Oct-4 levels upon infection, but a significant difference was observed in Nanog and Pax6 levels (Fig. 25). The increase in Pax6

levels upon adenoviral infection in both standard and KAP1 knockdown iPS cells might be due to the disruption of PML-NBs structure by adenovirus. PML bodies are known to be involved in regulating pluripotency (Hadjimichael et al. 2017). We know that upon infection, E4orf3 viral protein changes PML bodies' structure to track like (Doucas et al. 1996), and it has also been shown that *Pml*$^{-/-}$ iPSC expresses higher levels of Pax6 (Hadjimichael et al. 2017). We observed a decrease in the Nanog levels upon adenoviral infection. We know that Sox2 and Oct-4 regulate Nanog, and recent reports have shown that PML bodies interact with Sox2 and Oct-4. Their expression decreases upon PML knockdown (Hadjimichael et al. 2017). So, the adenoviral infection may modulate Sox2 or Oct-4 via PML, which leads to a reduction of Nanog levels. Adenovirus early protein E2A represents the replication centers of the virus, and HAdV places the sites of replication and transcription close to PML tracks (Stubbe et al., 2020). SUMOylation of a viral protein E2A governs the formation and localization of these PML tracks. So, the Sumoylation process and PML bodies may modulate the pluripotency of iPS cells upon adenoviral infection, but further experiments will be required to comment on this like the use of an shPML cell line or E2A SUMOylation defective cell line.

From the qPCR results, we saw that adenoviral infection decreases Nanog levels and increases Pax6 levels. Usually, Nanog level decreases upon differentiation. Also, overexpression of Pax6 restricts cell proliferation (Ouyang et al. 2006). Jang and Goldman showed that expression of Pax6 is enough to trigger a neurogenic destiny in glial progenitors (Jang and Goldman 2011), so we can speculate that adenoviral infection is pushing the iPS cells into differentiation. We think that E4orf3 and E2A are modulating Pax6 levels by disrupting PML structures, so we stained E4orf3, E2A, and Pax6 to check their localization. From the IF studies, we saw that E2A and E4orf3 staining is mostly nuclear. We also understand that Pax6 is getting concentrated in infected cells (Fig. 26). Pax6 overexpression is linked to many ocular defects like retinal dysplasia, microphthalmia (Manuel et al. 2008), and HAdV, also found to target eyes (Gonçalves and de Vries, 2006). Recently, Adeno associated vectors are highly used for retinal therapy; it raises concerns on the use of adeno associated vectors for gene therapy. Further experiments should be done to check the side effects of using AAV for gene therapy.

To sum up, our research highlights the role of KAP1 in the regulation of HERVs and pluripotency in iPS cells. We have tried to understand how adenoviral proteins modulate KAP1 and cause a change in HERVs and pluripotency levels. It also highlights the importance of PTMs and tissue-specific regulation of these factors.

Selected References:

- Ahi, Y.S., and Mittal, S.K. (2016). Components of adenovirus genome packaging. Front. Microbiol. *7*, 1503.
- Araujo, F.D., Stracker, T.H., Carson, C.T., Lee, D.V., and Weitzman, M.D. (2005). Adenovirus type 5 E4orf3 protein targets the Mre11 complex to cytoplasmic aggresomes. J. Virol. *79*, 11382–11391.
- Assinger, A., Yaiw, K.-C., Göttesdorfer, I., Leib-Mösch, C., and Söderberg-Nauclér, C. (2013). Human cytomegalovirus (HCMV) induces human endogenous retrovirus (HERV) transcription. Retrovirology *10*, 132.
- Bos, J.L., and ten Wolde-Kraamwinkel, H.C. (1983). The E1b promoter of Ad12 in mouse L tk- cells is activated by adenovirus region E1a. EMBO J. *2*, 73–76.
- Bürck, C., Mund, A., Berscheminski, J., Kieweg, L., Müncheberg, S., Dobner, T., and Schreiner, S. (2016). KAP1 Is a Host Restriction Factor That Promotes Human Adenovirus E1B-55K SUMO Modification. J. Virol. *90*, 930–946.
- Buzdin, A.A., Prassolov, V., and Garazha, A.V. (2017). Friends-Enemies: Endogenous Retroviruses Are Major Transcriptional Regulators of Human DNA. Front. Chem. *5*, 35.
- Buzdin, A., Kovalskaya-Alexandrova, E., Gogvadze, E., and Sverdlov, E. (2006). At least 50% of human-specific HERV-K (HML-2) long terminal repeats serve in vivo as active promoters for host nonrepetitive DNA transcription. J. Virol. *80*, 10752–10762.
- Chang, C.-W., Chou, H.-Y., Lin, Y.-S., Huang, K.-H., Chang, C.-J., Hsu, T.-C., and Lee, S.-C. (2008). Phosphorylation at Ser473 regulates heterochromatin protein 1 binding and corepressor function of TIF1beta/KAP1. BMC Mol. Biol. *9*, 61.
- Cheng, C.-T., Kuo, C.-Y., and Ann, D.K. (2014). KAPtain in charge of multiple missions: Emerging roles of KAP1. World J. Biol. Chem. *5*, 308–320.
- Chen, S., and Tian, X. (2018). Vaccine development for human mastadenovirus. J. Thorac. Dis. *10*, S2280–S2294.
- Cossec, J.-C., Theurillat, I., Chica, C., Búa Aguín, S., Gaume, X., Andrieux, A., Iturbide, A., Jouvion, G., Li, H., Bossis, G., et al. (2018). SUMO safeguards somatic and pluripotent cell identities by enforcing distinct chromatin states. Cell Stem Cell *23*, 742-757.e8.
- Davison, A.J., Benkő, M., and Harrach, B. (2003). Genetic content and evolution of adenoviruses. J. Gen. Virol. *84*, 2895–2908.
- Dobner, T., Horikoshi, N., Rubenwolf, S., and Shenk, T. (1996). Blockage by adenovirus E4orf6 of transcriptional activation by the p53 tumor suppressor. Science *272*, 1470–1473.
- Fields, B.N., Knipe, D.M., Chanock, R.M., Hirsch, M.S., Melnick, J.L., Monath, T.P., and Roizman, B. (1993). Fields virology. Rev. Inst. Med. Trop. S. Paulo *35*, 218–218.
- Gonçalves, M.A.F.V., and de Vries, A.A.F. (2006). Adenovirus: from foe to friend. Rev. Med. Virol. *16*, 167–186.

- Grandi, N., and Tramontano, E. (2018). HERV envelope proteins: physiological role and pathogenic potential in cancer and autoimmunity. Front. Microbiol. *9*, 462.
- Gupta, R., Michaud, H.-A., Zeng, X., Debbaneh, M., Arron, S.T., Jones, R.B., Ormsby, C.E., Nixon, D.F., and Liao, W. (2014). Diminished humoral responses against and reduced gene expression levels of human endogenous retrovirus-K (HERV-K) in psoriasis. J. Transl. Med. *12*, 256.
- Hadjimichael, C., Chanoumidou, K., Nikolaou, C., Klonizakis, A., Theodosi, G.-I., Makatounakis, T., Papamatheakis, J., and Kretsovali, A. (2017). Promyelocytic leukemia protein is an essential regulator of stem cell pluripotency and somatic cell reprogramming. Stem Cell Reports *8*, 1366–1378.
- Hoeben, R.C., and Uil, T.G. (2013). Adenovirus DNA replication. Cold Spring Harb. Perspect. Biol. *5*, a013003.
- Iyengar, S., and Farnham, P.J. (2011). KAP1 protein: an enigmatic master regulator of the genome. J. Biol. Chem. *286*, 26267–26276.
- Katzourakis, A., and Tristem, M. Phylogeny of Human Endogenous and Exogenous Retroviruses.
- King, C.A., Li, X., Barbachano-Guerrero, A., and Bhaduri-McIntosh, S. (2015). STAT3 Regulates Lytic Activation of Kaposi's Sarcoma-Associated Herpesvirus. J. Virol. *89*, 11347–11355.
- Kosulin, K., Haberler, C., Hainfellner, J.A., Amann, G., Lang, S., and Lion, T. (2007). Investigation of adenovirus occurrence in pediatric tumor entities. J. Virol. *81*, 7629–7635.
- Lallemand-Breitenbach, V., and de Thé, H. (2018). PML nuclear bodies: from architecture to function. Curr. Opin. Cell Biol. *52*, 154–161.
- Leppard, K.N. (2014). Adenoviruses: Molecular Biology☆. In Reference Module in Biomedical Sciences, (Elsevier), p.
- Lin, D., Tatham, M.H., Yu, B., Kim, S., Hay, R.T., and Chen, Y. (2002). Identification of a substrate recognition site on Ubc9. J. Biol. Chem. *277*, 21740–21748.
- Lion, T. (2014). Adenovirus infections in immunocompetent and immunocompromised patients. Clin. Microbiol. Rev. *27*, 441–462.
- Mager, D.L., and Medstrand, P. (2001). Retroviral Repeat Sequences. In Encyclopedia of Life Sciences, John Wiley & Sons, Ltd, ed. (Chichester: John Wiley & Sons, Ltd), p.
- Marion, M.-J., Hantz, O., and Durantel, D. (2010). The HepaRG cell line: biological properties and relevance as a tool for cell biology, drug metabolism, and virology studies. Methods Mol. Biol. *640*, 261–272.
- Misra, A., Chosdol, K., Sarkar, C., Mahapatra, A.K., and Sinha, S. (2001). Alteration of a sequence with homology to human endogenous retrovirus (HERV-K) in primary human glioma: implications for viral repeat mediated rearrangement. Mutation Research/Fundamental and Molecular Mechanisms of Mutagenesis *484*, 53–59.

- Muller, S., and Dobner, T. (2008). The adenovirus E1B-55K oncoprotein induces SUMO modification of p53. Cell Cycle *7*, 754–758.
- Nemerow, G.R., Pache, L., Reddy, V., and Stewart, P.L. (2009). Insights into adenovirus host cell interactions from structural studies. Virology *384*, 380–388.
- Okada, A., and Iwatani, Y. (2016). APOBEC3G-Mediated G-to-A Hypermutation of the HIV-1 Genome: The Missing Link in Antiviral Molecular Mechanisms. Front. Microbiol. *7*, 2027.
- Oleksiewicz, U., Gładych, M., Raman, A.T., Heyn, H., Mereu, E., Chlebanowska, P., Andrzejewska, A., Sozańska, B., Samant, N., Fąk, K., et al. (2017). TRIM28 and Interacting KRAB-ZNFs Control Self-Renewal of Human Pluripotent Stem Cells through Epigenetic Repression of Pro-differentiation Genes. Stem Cell Reports *9*, 2065–2080.
- Osumi, N., Shinohara, H., Numayama-Tsuruta, K., and Maekawa, M. (2008). Concise review: Pax6 transcription factor contributes to both embryonic and adult neurogenesis as a multifunctional regulator. Stem Cells *26*, 1663–1672.
- Rauwel, B., Jang, S.M., Cassano, M., Kapopoulou, A., Barde, I., and Trono, D. (2015). Release of human cytomegalovirus from latency by a KAP1/TRIM28 phosphorylation switch. Elife *4*.
- Reverter, D., and Lima, C.D. (2005). Insights into E3 ligase activity revealed by a SUMO-RanGAP1-Ubc9-Nup358 complex. Nature *435*, 687–692.
- Rowe, H.M., and Trono, D. (2011). Dynamic control of endogenous retroviruses during development. Virology *411*, 273–287.
- Rowe, H.M., Jakobsson, J., Mesnard, D., Rougemont, J., Reynard, S., Aktas, T., Maillard, P.V., Layard-Liesching, H., Verp, S., Marquis, J., et al. (2010). KAP1 controls endogenous retroviruses in embryonic stem cells. Nature *463*, 237–240.
- Rowe, W.P., Huebner, R.J., Gilmore, L.K., Parrott, R.H., and Ward, T.G. (1953). Isolation of a cytopathogenic agent from human adenoids undergoing spontaneous degeneration in tissue culture. Proc. Soc. Exp. Biol. Med. *84*, 570–573.
- Saha, B., Wong, C.M., and Parks, R.J. (2014). The adenovirus genome contributes to the structural stability of the virion. Viruses *6*, 3563–3583.
- Sarnow, P., Ho, Y.S., Williams, J., and Levine, A.J. (1982a). Adenovirus E1b-58kd tumor antigen and SV40 large tumor antigen are physically associated with the same 54 kd cellular protein in transformed cells. Cell *28*, 387–394.
- Schlesinger, S., and Goff, S.P. (2015). Retroviral transcriptional regulation and embryonic stem cells: war and peace. Mol. Cell. Biol. *35*, 770–777.
- Schreiner, S., Wimmer, P., Sirma, H., Everett, R.D., Blanchette, P., Groitl, P., and Dobner, T. (2010). Proteasome-dependent degradation of Daxx by the viral E1B-55K protein in human adenovirus-infected cells. J. Virol. *84*, 7029–7038.
- Schreiner, S., Wimmer, P., Groitl, P., Chen, S.-Y., Blanchette, P., Branton, P.E., and Dobner, T. (2011). Adenovirus type 5 early region 1B 55K oncoprotein-dependent degradation of cellular factor Daxx is required for efficient transformation of primary rodent cells. J. Virol. *85*, 8752–8765.

- Schreiner, S., Martinez, R., Groitl, P., Rayne, F., Vaillant, R., Wimmer, P., Bossis, G., Sternsdorf, T., Marcinowski, L., Ruzsics, Z., et al. (2012). Transcriptional activation of the adenoviral genome is mediated by capsid protein VI. PLoS Pathog. *8*, e1002549.
- Shah, G.A., and O'Shea, C.C. (2015). Viral and cellular genomes activate distinct DNA damage responses. Cell *162*, 987–1002.
- Shi, G., and Jin, Y. (2010). Role of Oct4 in maintaining and regaining stem cell pluripotency. Stem Cell Res. Ther. *1*, 39.
- Sohn, S.-Y., and Hearing, P. (2016). Adenovirus early proteins and host sumoylation. MBio *7*.
- Stoll, G.A., Oda, S.-I., Chong, Z.-S., Yu, M., McLaughlin, S.H., and Modis, Y. (2019). Structure of KAP1 tripartite motif identifies molecular interfaces required for retroelement silencing. Proc Natl Acad Sci USA *116*, 15042–15051.
- Stoye, J.P. (2012). Studies of endogenous retroviruses reveal a continuing evolutionary saga. Nat. Rev. Microbiol. *10*, 395–406.
- Stubbe, M., Mai, J., Paulus, C., Stubbe, H.C., Berscheminski, J., Karimi, M., Hofmann, S., Weber, E., Hadian, K., Hay, R., et al. (2020). Viral DNA binding protein sumoylation promotes PML nuclear body localization next to viral replication centers. MBio *11*.
- Suntsova, M., Garazha, A., Ivanova, A., Kaminsky, D., Zhavoronkov, A., and Buzdin, A. (2015). Molecular functions of human endogenous retroviruses in health and disease. Cell. Mol. Life Sci. *72*, 3653–3675.
- Tang, L., An, J., Xie, Z., Dehghan, S., Seto, D., Xu, W., and Ji, Y. (2013). Genome and bioinformatic analysis of a HAdV-B14p1 virus isolated from a baby with pneumonia in Beijing, China. PLoS ONE *8*, e60345.
- Turelli, P., Castro-Diaz, N., Marzetta, F., Kapopoulou, A., Raclot, C., Duc, J., Tieng, V., Quenneville, S., and Trono, D. (2014). Interplay of TRIM28 and DNA methylation in controlling human endogenous retroelements. Genome Res. *24*, 1260–1270.
- Vetrini, F., and Ng, P. (2010). Gene therapy with helper-dependent adenoviral vectors: current advances and future perspectives. Viruses *2*, 1886–1917.
- White, D., Rafalska-Metcalf, I.U., Ivanov, A.V., Corsinotti, A., Peng, H., Lee, S.-C., Trono, D., Janicki, S.M., and Rauscher, F.J. (2012). The ATM substrate KAP1 controls DNA repair in heterochromatin: regulation by HP1 proteins and serine 473/824 phosphorylation. Mol. Cancer Res. *10*, 401–414.
- Williams, J., Williams, M., Liu, C., and Telling, G. (1995). Assessing the role of E1A in the differential oncogenicity of group A and group C human adenoviruses. Curr. Top. Microbiol. Immunol. *199 (Pt 3)*, 149–175.
- Yang, J., Yu, Y., Hamrick, H.E., and Duerksen-Hughes, P.J. (2003). ATM, ATR and DNA-PK: initiators of the cellular genotoxic stress responses. Carcinogenesis *24*, 1571–1580.
- Yousuf, M.A., Zhou, X., Mukherjee, S., Chintakuntlawar, A.V., Lee, J.Y., Ramke, M., Chodosh, J., and Rajaiya, J. (2013). Caveolin-1 associated adenovirus entry into human corneal cells. PLoS ONE *8*, e77462.

- Zhang, Q., Jing, S., Cheng, Z., Yu, Z., Dehghan, S., Shamsaddini, A., Yan, Y., Li, M., and Seto, D. (2017). Comparative genomic analysis of two emergent human adenovirus type 14 respiratory pathogen isolates in China reveals similar yet divergent genomes. Emerg. Microbes Infect. *6*, e92.
- Zhang, W., Low, J.A., Christensen, J.B., and Imperiale, M.J. (2001). Role for the adenovirus IVa2 protein in packaging of viral DNA. J. Virol. *75*, 10446–10454.
- Zhong, S., Salomoni, P., and Pandolfi, P.P. (2000). The transcriptional role of PML and the nuclear body. Nat. Cell Biol. *2*, E85-90.